

SAMPLE AND HOLD FUNCTIONS AND NON-MINIMUM-PHASE SYSTEMS

By

Yingxu Wang

A THESIS

Submitted to  
Michigan State University  
in partial fulfillment of the requirements  
for the degree of

Engineering Mechanics – Master of Science

2014

# **ABSTRACT**

## **SAMPLE AND HOLD FUNCTIONS AND NON-MINIMUM-PHASE SYSTEMS**

By

Yingxu Wang

With the same initial condition, a continuous-time system and the corresponding DE system will have the same system responses at sampling times due to switched input and zero-order hold input, respectively. A previous work had been done to show that using the Square Pulse Sample and Hold Function (SPSHF) as the switched input, the corresponding Discrete Equivalent (DE) system of a continuous-time non-minimum phase (NMP) system could have minimum phase (MP) behavior. In this thesis, the switched input in the definition of DE system was expended with another two sample and hold functions, Forward Triangle Sample and Hold Function (FTSHF) and Backward Triangle Sample and Hold Function (BTSHF). The DE systems and its Discrete Time (DT) systems equations were developed according to different sample and hold functions. A simulation case study was proceeded to indicate the feasible regions for selecting the sample and hold parameters for each switched input, which would lead the resulting DE systems MP. The results of simulation case study implied that it was possible to have an MPDT system with a smaller sampling period than discretizing the system directly using zero-order hold (ZOH) method. In order to study the robustness of each sample and hold function, the q-Markov cover system identification with Pseudo Random Binary Signal (PRBS) was then studied for the purpose of doing controller-in-the-loop (CIL) simulation. The CIL simulation used the dSPACE auto-box to simulate the system dynamics. A resistant-capacitor (RC) filter was used to simulate actuator dynamics using different capacitors. At last the characteristics of the three sample and hold functions were compared.

## ACKNOWLEDGEMENTS

Two years had passed as if it was only two days. I can still remember the day that I knocked at the door of Dr. Zhu's office, he welcomed me with a warm smile that made me feel like he was only an old friend but not a professor. Actually we did become friends. I really appreciated the wisdom choice I made to be Dr. Zhu's student. He treated his students as his children, he thought what we thought and he felt what we felt. With his generous and patient guidance, I finished my master thesis research. He also led me into the whole new area of control by inspiring me to be confident. He was always saying that "control is not a course or degree, it is more about art, we can achieve the same goal in a thousand ways, and maybe none of them is wrong. What we do is to enjoy the process." This was what I learned during my way to graduation and I really appreciated that. To be his student is my honor, my luck, and also my destiny. Here, all I want to say is thank you.

I would also like to thank my committee members: Dr. Ranjan Mukherjee, who provided the fundamental reference and help. He treated me as his buddy and supported me in both my study and my life; Dr. Jongeun Choi, my first professor, who gave me the introduction of control, and is always willing to help. Thank you for your help and support.

Without my friends in the lab, I could hardly imagine how hard my research will be. My appreciation is also for you: Shupeng Zhang, Jie Yang, Tao Zeng, Hailiang Zheng, and Jerry Yang.

Also, I would like to thank my girlfriend Changchang Yao for everything she did. She pointed a way when I feel it was dark everywhere. She made me to believe I could do everything, not for anyone, but for myself.

Last but not least, to my parents: it was them, who supported me to finish my four years collage and my two years graduate school. They know nothing about control, they did not even know what mechanical engineering is about, but they could understand whether I'm suffering or happy. They supported me without saying a word, but I could understand.

Actually I could never finish my acknowledgement in such few words. I simply wish everyone healthy and enjoy their lives.

# TABLE OF CONTENTS

LIST OF TABLES .....	vii
LIST OF FIGURES .....	viii
CHAPTER 1 INTRODUCTION .....	1
1.1 Background and Motivation.....	1
1.2 Research Overview .....	2
1.3 Organization .....	4
CHAPTER 2 DE SYSTEMS WITH THREE SAMPLE AND HOLD FUNCTIONS .....	5
2.1 DE System and the SPSHF .....	5
2.2 The FTSHF and the Associate DE System .....	7
2.3 The BTSHF and the Associate DE System .....	8
2.4 The DT Systems .....	10
CHAPTER 3 A SIMULATION CASE STUDY .....	12
3.1 DT System with the SPSHF .....	13
3.2 DT System with the FTSHF.....	14
3.3 DT System with the BTSHF .....	16
3.4 Analysis .....	17
CHAPTER 4 Q-MARKOV COVER IDENTIFICATION USING PRBS INPUT .....	20
4.1 Introduction .....	20
4.2 PRBS Used for Q-Markov Cover.....	22
4.3 System Identification.....	25
4.3.1 System Identification Steps.....	25
4.3.2 System Identification Parameter Determination.....	27
4.3.3 Identification Result of the SPSHF Case .....	30
4.3.4 Identification Result of the FTSHF Case .....	31
4.3.5 Identification Result of the BTSHF Case .....	32
4.4 DE System GUI for finding the DE systems.....	33
4.4.1 Introduction.....	33
4.4.2 Procedure .....	34
4.4.3 Benefits .....	35
4.4.4 Future Work of the DE GUI .....	36
CHAPTER 5 CIL SIMULATION USING A DSPACE AUTO-BOX .....	38
5.1 Introduction .....	38
5.2 RC Filter .....	42

5.3 CIL Result .....	44
5.4 Analysis .....	46
CHAPTER 6 CONCLUSIONS .....	48
BIBLIOGRAPHY .....	50

## LIST OF TABLES

TABLE 1. Coefficients for maximum sequences .....	23
TABLE 2. The pole and zero absolute value of the SPSHF-DT case .....	31
TABLE 3. The pole and zero absolute value of the FTSHF-DT case .....	32
TABLE 4. The pole and zero absolute value of the BTSHF-DT case .....	33
TABLE 5. Time constant VS. pole locations .....	43

## LIST OF FIGURES

Figure 1. The flowchart of MPDT system achieving process .....	3
Figure 2. Continuous input, ZOSHF and three switched sample and hold functions .....	5
Figure 3. A continuous-time system match with its DE system at sampling times.....	7
Figure 4. Maximum zero of the SPSHF-DT system VS. sample and hold parameters.....	13
Figure 5. Pole zero plot of the SPSHF-DT system .....	14
Figure 6. Maximum zero of the FTSHF-DT system VS. sample and hold parameters.....	15
Figure 7. Pole zero plot of the FTSHF-DT system.....	16
Figure 8. Maximum zero of the BTSHF-DT system VS. sample and hold parameters .....	16
Figure 9. Pole zero plot of the BTSHF-DT system .....	17
Figure 10. Regions of all the sample and hold functions for selecting the switch parameters so that the resulting DT system is MP .....	18
Figure 11. The layout of system identification using PRBS input .....	21
Figure 12. Several periods of PRBS signal with the order of 11 .....	24
Figure 13. The modified PRBS signal .....	24
Figure 14. System response due to different inputs .....	25
Figure 15. Simulation layout.....	28
Figure 16. System Identification GUI .....	29
Figure 17. The pole-zero plot of SPSHF-DT, identified and NMP systems .....	30
Figure 18. The pole-zero plot of FTSHF-DT, identified and NMP systems .....	31
Figure 19. The pole-zero plot of BTSHF-DT, identified and NMP systems.....	32



Figure 20. The GUI for finding the MPDT system .....	37
Figure 21. The flowchart of CIL Simulation .....	39
Figure 22. dSPACE setup .....	40
Figure 23. dSPACE control desk layout .....	41
Figure 24. The modified PRBS input signal .....	44
Figure 25. The zero moving trend of the identified system with SPSHF .....	45
Figure 26. The zero moving trend of the identified system with FTSHF .....	45
Figure 27. The zero moving trend of the identified system with BTSHF .....	46
Figure 28. Overall zero moving trends of the three sample and hold functions .....	47

# CHAPTER 1

## INTRODUCTION

### 1.1 Background and Motivation

From transfer function point of view, in continuous-time domain, a NMP system is a plant that has at least one zero locates in the right hand plan (RHP). And in discrete-time domain, a NMP system has at least one zero locates outside of the unit circle. NMP system could be seen everywhere in real life, including aircraft, hydraulic turbines, automotive continuously variable transmissions, and so on [1]. People are always trying to avoid NMP characteristics when considering a control method because of the problems caused by the unstable zeroes. Including slow step response with large undershoot and an additional phase shift and excessive phase lag with no attenuation at high frequencies [2]. During a control process, when a PI or PID controller is applied to a NMP system, when necessary, a proportional gain may be very large, from the aspect of Root Locus, when the proportional gain increases, the closed loop poles will move toward the open loop zeroes, which may change the stability of the NMP system. So when a NMP system is in the loop, prevent high gain control is applied, which leads to poor close-loop performance [1].

In order to control NMP systems, several methods are studied [2]-[10] before. For example, the fuzzy control was studied in [2] and [3] to eliminate the undershot in order to change the transient response. In [4] an artificial neural network was studied to achieve improving the NMP system performance. The genetic algorithm was used for off-line training in the artificial neural network. In [5] a new method called direct adaptive control structure came up for controlling the NMP systems. According to this result, the direct adaptive control method was also developed

for not necessarily MP systems based on simultaneous identification when using the input and output of a prediction models [6]. Another method called variable structure system [7] was used for controlling a NMP system by assigning the pole to achieve model reference control. The last one, which is more close to the area researched in this thesis, an alternative approach presented in [8], shows the study of DE system characteristics with a sample and hold function, different from the zero order holding one. It specifically introduced the SPSHF. It had been validated that a proper choice of sampling period and pulse duty cycle, it could make the DE system of a NMP system become MP. In this thesis, a stable NMP system was studied as a numerical example. Also in [9], it is found that a continuous time NMP system could be MP when discretizing the system directly with zero-order hold method with a certain sampling rate. The theory from this thesis will make the largest sampling rate for directly discretizing with zero-order hold even larger.

## **1.2 Research Overview**

In [8], the SPSHF was defined as the switched input for achieving the DE analytical state space matrix equations. In this thesis, the switched input definition is expended with another two sample and hold functions: FTSHF and BTSHF, and the corresponding DE equations are derived in the same way as in [8].

When a different sample and hold function method is applied, the corresponding DE system has the same poles, but the zeroes locate differently. Also, for the same sample and hold function method, when the sample and hold parameters change, the zeroes moves accordingly. According to this, it is possible to have the DE and DT of a NMP system to be MP. In the following flowchart (figure 1), the process of obtaining a MPDT system of a NMP is shown.

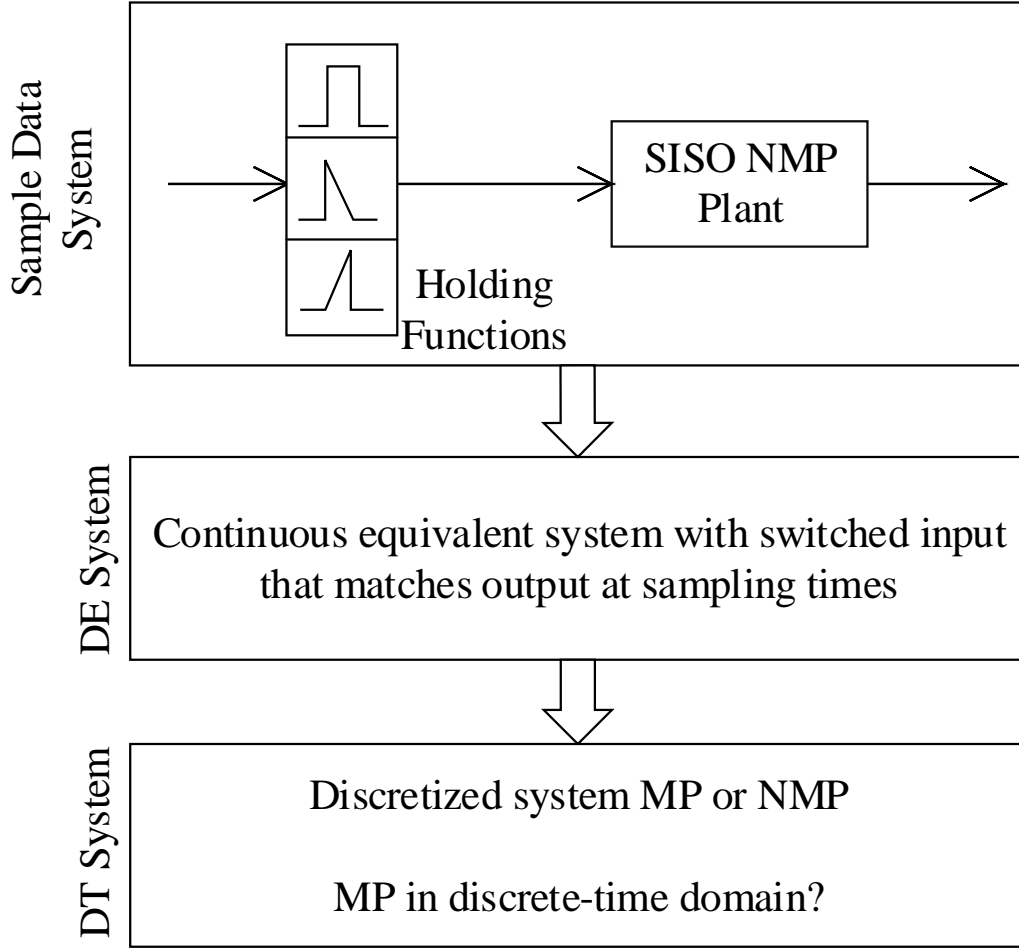


Figure 1. The flowchart of MPDT system achieving process

This method has its advantage of convenience which is no more need to study any methods of controlling a NMP system with trying to avoid the negative effects of the system, but find the MP DE system of the NMP system to determine the switched input, instead of studying the NMP system itself.

However, this method has its disadvantage. According to different requirements, when the duty cycle reduce, a large actuator with faster response time is needed, which means that the energy cost may increase. As the limitation of actuator, the selection of the sample and hold function duty cycle cannot be arbitrary small.

The main contribution of this thesis is to study the switched input of a NMP system. By adjusting the sample and hold parameters, the NMP system could have MP characteristics.

### **1.3 Organization**

The paper is organized as follows. Chapter II showed how the DE analytical state space matrix equations with three sample and hold functions were driven. In chapter III, the properties of the MPDE systems were studied, and also the DT systems. A numerical example showed how to select sample and hold parameters for different sample and hold functions. In the next chapter, system identification was studied as a tool for of doing controller-in-the-loop (CIL) simulation. And also a built GUI was showed in order to make the calculation process simpler. Chapter V was testing the robustness of this theory with a CIL real-time simulation. dSPACE auto-box was used to be the hardware in the loop. The last chapter added some conclusions.

## CHAPTER 2

### DE SYSTEMS WITH THREE SAMPLE AND HOLD FUNCTIONS

#### 2.1 DE System and the SPSHF

Consider the continuous time input  $u(t)$  shown in Figure 2. (a). The input can be discretized using Zero-Order Sample and Hold Function (ZOSHF) with the sampling period of  $\delta$  and represented by  $\hat{u}(t)$  shown in Figure 2. (b). Base on the ZOSHF, the switched input is the SFSHF, shown in Figure 2. (c).

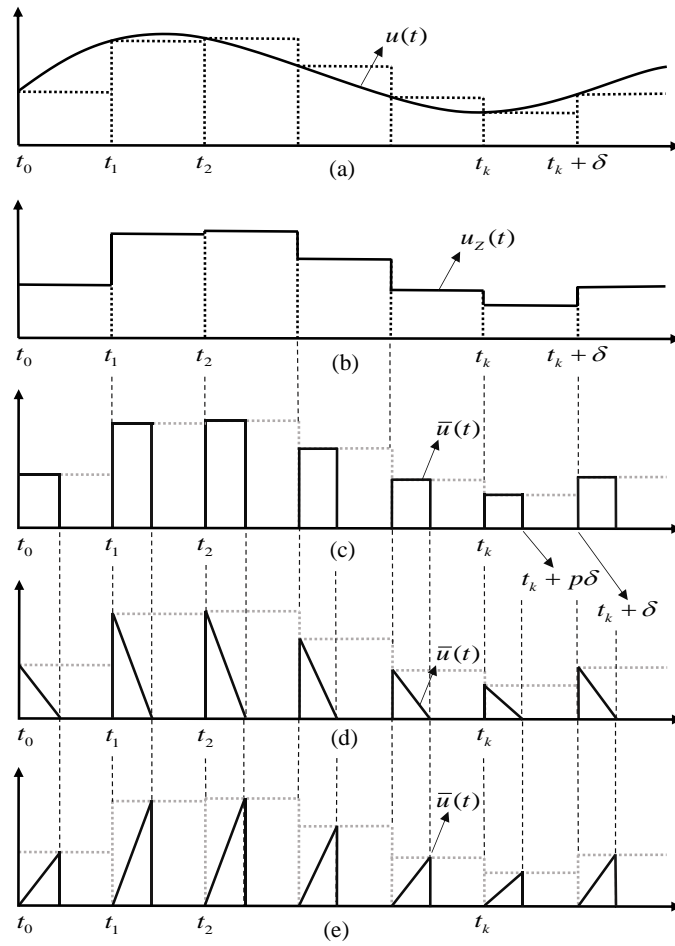


Figure 2. Continuous input, ZOSHF and three switched sample and hold functions

The switched input  $\bar{u}(t)$  described in Figure 2. (c) is SFSHF and defined as

$$\bar{u}(t) = \begin{cases} u_z(t_k), & \text{if } t_k < t < t_k + p\delta \\ 0, & \text{if } t_k + p\delta < t < t_k + \delta \end{cases} \quad (1)$$

$k = 0, 1, 2, \dots$

In which  $u_z(t_k)$  is the ZOH value of  $u(t_k)$  over the interval  $[t_k, t_k + \delta]$  (shown in Figure 2. (b)), and  $\delta \in (0, \infty)$  is the sample period of the input pulse,  $p \in (0, 1]$  is the duty cycle. Consider the linear system in (2).

$$\begin{aligned} \dot{x}(t) &= Ax(t) + B\bar{u}(t), \quad x(t_0) = x_0 \\ y(t) &= Cx(t) \end{aligned} \quad (2)$$

With the switched input in (1), the state variables at sampling times are defined as:

$$\begin{aligned} x(t_k + p\delta) &= e^{Ap\delta} x(t_k) + \int_0^{p\delta} e^{A(p\delta - \tau)} B\bar{u}(t_k + \tau) d\tau \\ &= e^{Ap\delta} x(t_k) + A^{-1}(e^{Ap\delta} - I)Bu(t_k) \\ x(t_{k+1}) &= e^{A(\delta - p\delta)} x(t_k + p\delta) \\ &= e^{A\delta} x(t_k) + A^{-1}(e^{A\delta} - e^{A(1-p)\delta})Bu(t_k) \end{aligned} \quad (3)$$

According to [10], the definition of DE system is defined as:

**Definition 1** (DE): a continuous time system:

$$\begin{aligned} \dot{\bar{x}}(t) &= \bar{A}\bar{x}(t) + \bar{B}u_z(t), \quad \bar{x}(t_0) = x_0 \\ \bar{y}(t) &= \bar{C}\bar{x}(t) \end{aligned} \quad (4)$$

which has the state variables at sampling times  $t_k + \delta$  are given by

$$\begin{aligned} \bar{x}(t_{k+1}) &= e^{\bar{A}\delta} \bar{x}(t_k) + \int_0^{\delta} e^{\bar{A}(\delta - \tau)} \bar{B} u_z(t_k + \tau) d\tau \\ &= e^{\bar{A}\delta} \bar{x}(t_k) + \bar{A}^{-1}(e^{\bar{A}\delta} - I)\bar{B} u(t_k) \end{aligned} \quad (5)$$

is a DE system of system (2), if the state variables of (5) match with those in (3) at sampling times  $t_k, k = 0, 1, 2, \dots$ . This leads the state space matrices equation of DE system with the SPSHF:

$$\begin{aligned}\bar{A} &= A \\ \bar{B} &= [I - e^{-A\delta}]^{-1} [I - e^{-Ap\delta}] B \\ \bar{C} &= C\end{aligned}\tag{6}$$

The continuous time system with square pulse switched input and the corresponding DE system are shown in Figure 3. The Matching behavior is clearly showed as well.

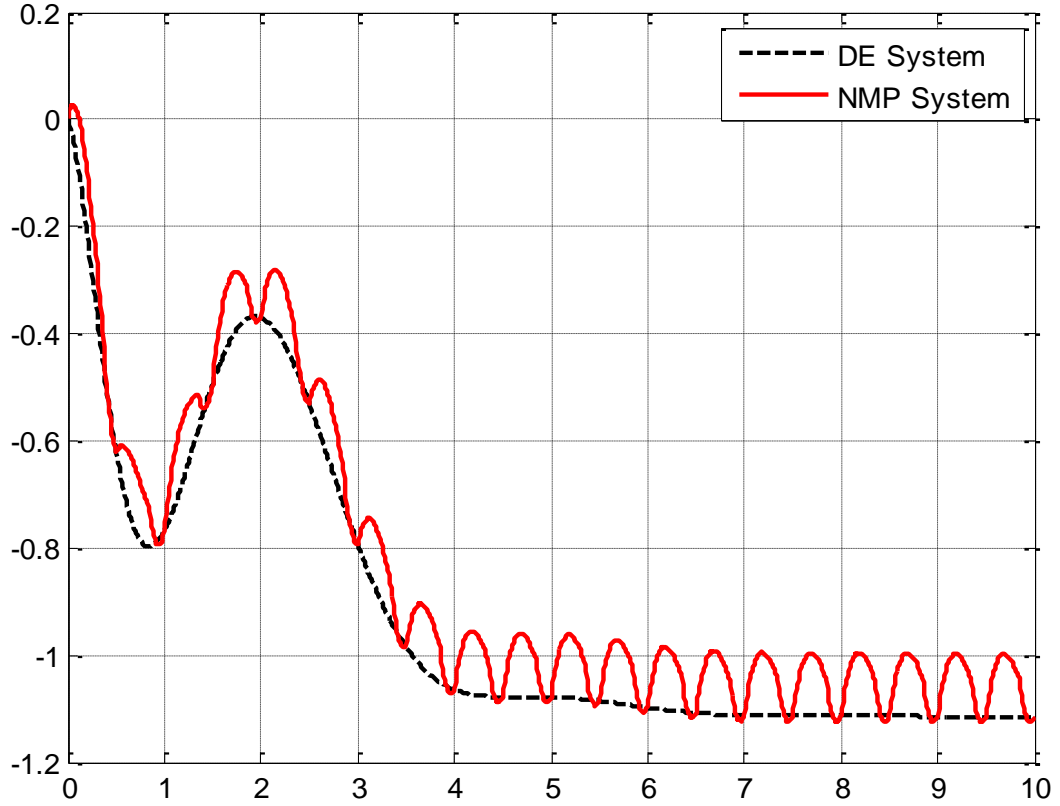


Figure 3. A continuous-time system match with its DE system at sampling times

## 2.2 The FTSHF and the Associated DE System



With the same concept, the switched input definition is changed from the SPSHF to the FTSHF and shown in Figure 2. (d). and defined is defined as:

$$\bar{u}(t) = \begin{cases} \frac{u_z(t)(t_k - t)}{p\delta} + u_z(t), & \text{if } t_k < t < t_k + p\delta \\ 0, & \text{if } t_k + p\delta < t < t_k + \delta \end{cases} \quad (7)$$

$k = 0, 1, 2, \dots$

In where  $\delta \in (0, \infty)$  is the sampling period,  $p \in (0, 1]$  is the duty cycle of the switched input.

For the FTSHF, it is the same as SPSHF case: equaling the state variables of the original system (2) and the state variables of the DE system with FTSHF in (8):

$$\begin{aligned} x_{(t_k + p\delta)} &= e^{Ap\delta} x_k + \int_0^{p\delta} e^{A(p\delta - \tau)} \bar{B} \bar{u}(t_k + \tau) d\tau \\ &= e^{Ap\delta} x_k + 2A^{-1} \left( \frac{1}{p\delta} A^{-1} - \frac{1}{p\delta} A^{-1} e^{Ap\delta} + e^{Ap\delta} \right) \bar{B} \\ x_{(t_{k+1})} &= e^{A(\delta - (p\delta))} \bar{x}_{(t_k + p\delta)} \\ &= e^{A\delta} x_k + 2A^{-1} \left( \frac{1}{p\delta} A^{-1} e^{A(1-p)\delta} - \frac{1}{p\delta} A^{-1} e^{A\delta} + e^{A\delta} \right) \bar{B} \end{aligned} \quad (8)$$

The state space equation of DE system with the FTSHF is achieved:

$$\begin{aligned} \bar{A} &= A \\ \bar{B} &= (I - e^{-A\delta})^{-1} \left[ \frac{1}{p\delta} A^{-1} (e^{-Ap\delta} - I) + I \right] B \\ \bar{C} &= C \end{aligned} \quad (9)$$

### 2.3 The BTSHF and the Associated DE System

The last sample and hold function is the BTSHF which is shown in Fig. 2 (c) with dotted lines and defined as:

$$\bar{u}(t) = \begin{cases} \frac{(t-t_k)}{p\delta} u_z(t_k), & \text{if } t_k < t < t_k + p\delta \\ 0, & \text{if } t_k + p\delta < t < t_k + \delta \end{cases} \quad (10)$$

$k = 0, 1, 2, \dots$

The process of achieving DE system with the BTSHF is the same as the FTSHF, substitute (10) into (4), and the state variables are shown in (11):

$$\begin{aligned} \bar{x}_{(t_k+p\delta)} &= e^{A(t_k+p\delta-t_k)} x_k + \int_0^{p\delta} e^{A(p\delta-\tau)} \bar{B} u_z(t_k-\tau) d\tau \\ &= e^{A(p\delta)} x_k - \frac{2}{p\delta} p\delta A^{-1} B - \frac{2}{p\delta} A^{-2} B + \frac{2}{p\delta} A^{-2} e^{Ap\delta} \bar{B} \\ \bar{x}_{(t_{i+1})} &= e^{A(\delta-p\delta)} \bar{x}_{(t_k+p\delta)} \\ &= e^{A\delta} x_k + 2A^{-1} \left( -\frac{1}{p\delta} p\delta e^{A(1-p)\delta} - \frac{1}{p\delta} A^{-1} e^{A(1-p)\delta} + \frac{1}{p\delta} A^{-1} e^{A\delta} \right) \bar{B} \end{aligned} \quad (11)$$

The DE system equation with the BTSHF is obtained by equaling (11) and (5):

$$\begin{aligned} \bar{A} &= A \\ \bar{B} &= \left[ \frac{1}{p\delta} A^{-1} (I - e^{-Ap\delta}) - e^{-Ap\delta} \right]^{-1} (I - e^{-A\delta}) B \\ \bar{C} &= C \end{aligned} \quad (12)$$

From the equations of the DE systems (6), (9), and (12), DE system is related to the switched input with its sample and hold parameters. And it is obvious that the input  $\bar{u}(t)$  is canceled out, which means that the characteristics of the DE system only dependent on the sample and hold parameters. The first assumption is that the original system state space matrices are minimal realization from the system transfer function. According to this assumption and the equations of DE systems, the poles of the DE system and the original system should be identical because  $A = \bar{A}$ . And the zeroes are different because  $B \neq \bar{B}$ . And the  $\bar{B}$  matrix of the DE system is

varying with the two sample and hold parameters ( $\delta$  and  $p$ ). As a result, it is possible that if a specific combination of sample and hold parameters are chosen, the DE system could be MP.

## 2.4 The DT Systems

DT systems are achieved by discretizing the DE systems with zero order hold with the same sampling period as the switched inputs. Apparently, the DT systems, DE systems, and the original system will all have the same state variables at sampling times due to the same sample and hold parameters and sample and hold function. The state space form of the DT system is given by:

$$\begin{aligned} x(t_k + \delta) &= A_d x(t_k) + B_d u(t_k), \quad x(t_0) = x_0 \\ y(t_k) &= C_d x(t_k) \end{aligned} \quad (13)$$

For the SPSHF, the DT system is calculated is referred as the SFPSH-DT system, and is given by:

$$\begin{aligned} A_d &= e^{A\delta} \\ B_d &= M_p A^{-1} (e^{A\delta} - I) (I - e^{-A\delta})^{-1} (I - e^{-Ap\delta}) B \\ C_d &= C \end{aligned} \quad (14)$$

for the FTSHF-DT system:

$$\begin{aligned} A_d &= e^{A\delta} \\ B_d &= M_t A^{-1} (e^{A\delta} - I) (I - e^{-A\delta})^{-1} \left[ A^{-1} \frac{e^{-Ap\delta} - I}{p\delta} + I \right] B \\ C_d &= C \end{aligned} \quad (15)$$

and the BTSHF-DT system:

$$\begin{aligned}
A_d &= e^{A\delta} \\
B_d &= M_t A^{-1} (e^{A\delta} - I) (I - e^{-A\delta})^{-1} \left[ A^{-1} \frac{I - e^{-Ap\delta}}{p\delta} - e^{-Ap\delta} \right] B \\
C_d &= C
\end{aligned} \tag{16}$$

After discretization, the DT system with any sample and hold function described in this thesis has the same pole locations. However the zeroes could be quite different since the control input matrix  $\bar{B}_d$  of the DT system is different.

## CHAPTER 3

### A SIMULATION CASE STUDY

An example of a continuous-time, SISO, NMP system with the form of transfer function shown as below

$$G(s) = \frac{(s-5)(s^2+1)}{(s+2)(s+1)(s^2+2s+5)} \quad (17)$$

To calculate the DE and the DT systems with state variables, the state space form of the system has to be achieved. After minimal realization, the state space form of the system is

$$\begin{aligned} A &= \begin{bmatrix} 0 & 0 & 0 & -10 \\ 1 & 0 & 0 & -19 \\ 0 & 1 & 0 & -13 \\ 0 & 0 & 1 & -5 \end{bmatrix} & B &= \begin{bmatrix} -5 \\ 1 \\ -5 \\ 1 \end{bmatrix} \\ C &= [0 \quad 0 \quad 0 \quad 1] & D &= 0 \end{aligned} \quad (18)$$

During the simulation,  $\delta$  is bounded by 0 and 2. Since  $p$  is representing the duty cycle in percentage, it is bounded by 0 and 1. In order to determine the feasible  $\delta$  and  $p$  combination, 3-D plots in Figure 4, Figure 5, and Figure 8 of the DT systems with the three sample and hold functions are plotted. Z-axis is representing the max absolute value of the DT system, and X-Y plane is representing the sample and hold parameters. As a result, the DT system is MP when the max absolute zero is smaller than 1, hence the feasible regions for selecting the sample and hold parameters so that the resulting DT system is MP is the part under the  $z = 1$  plane.

### 3.1 DT System with the SPSHF

The 3-D plot of the SPAHF-DT system max zero distribution according to the sample and hold parameters is shown in Figure 4:

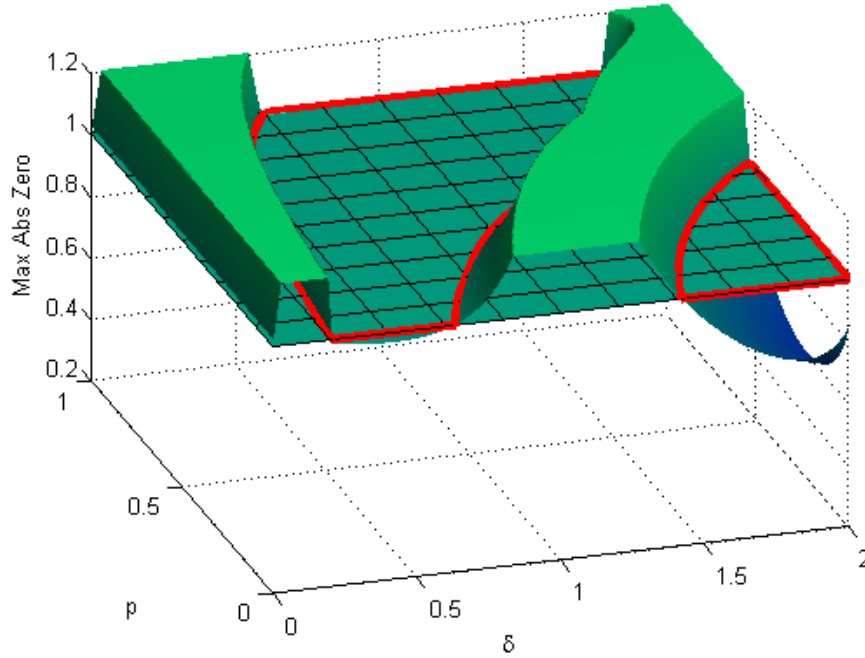


Figure 4. Maximum zero of the SPSHF-DT system VS. sample and hold parameters

In this 3-D plot, the feasible region for selecting the sample and hold parameters is within the red region. With the sample and hold parameter selected randomly,  $\delta = 0.5$ ,  $p = 0.4$ , the corresponding pole-zero plot is:

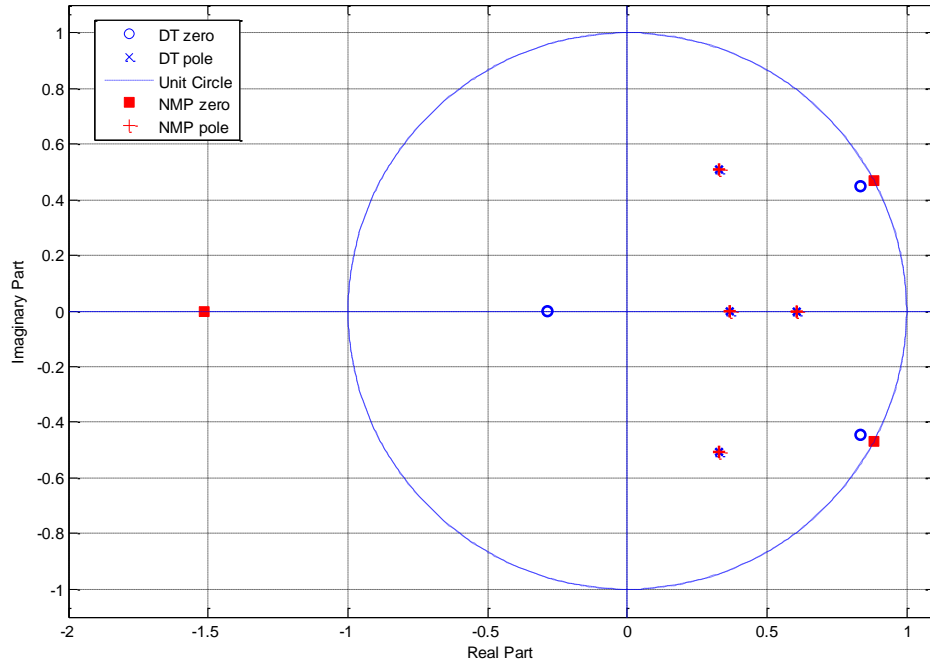


Figure 5 Pole zero plot of the SPSHF-DT system

The red dots represent the NMP system zeroes and poles, and the blue dots represent the DT system zeroes and poles. With this combination of the sample and hold parameters, the SPSHF-DT system is MP.

### 3.2 DT System with the FTSHF

The 3-D plot of the FTSHF case is shown in Figure 6:

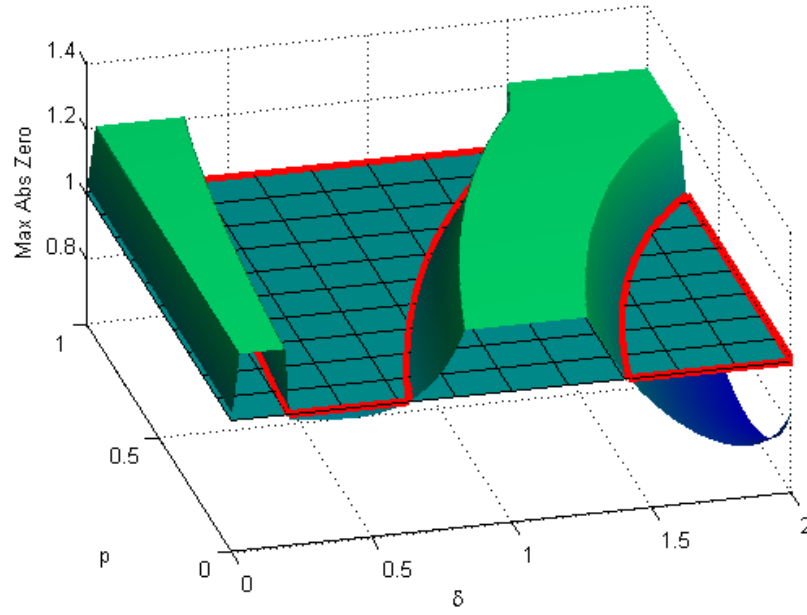


Figure 6. Maximum zero of the FTSHF-DT system VS. sample and hold parameters

It is obvious that the 3-D plot of the FTSHF-DT system is quite different from SPSHF-DT system. These two plots has different feasible regions for selecting the sample and hold parameters. With the sample and hold parameter selected randomly but inside the red region,  $\delta = 0.5, p = 0.3$ , the corresponding pole-zero plot is:



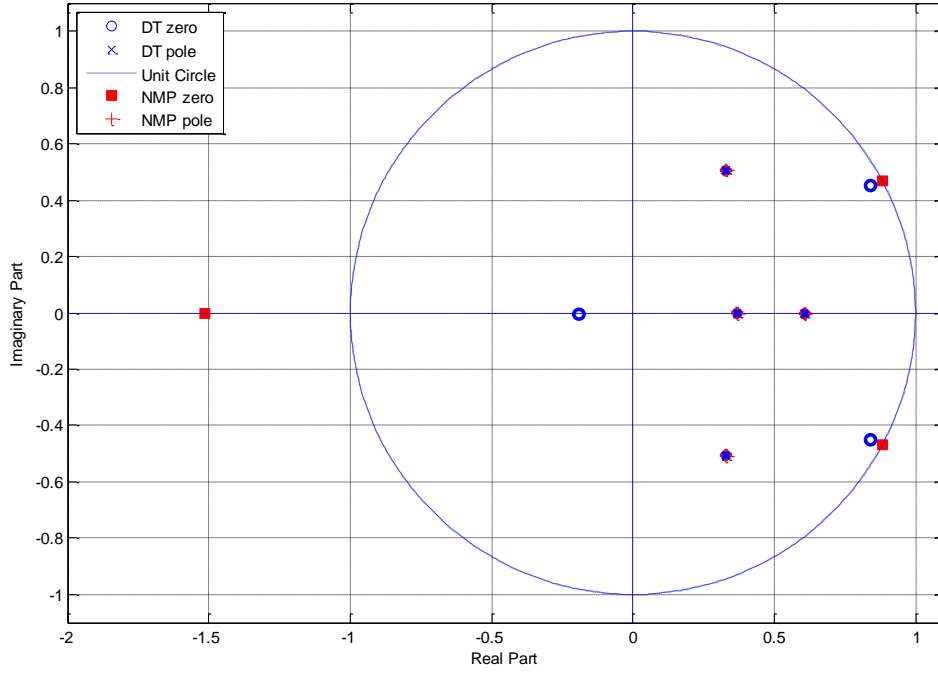


Figure 7. Pole zero plot of the FTSHF-DT system

### 3.3 DT System with the BTSHF

The 3-D plot of the BTSHF-DT system is shown in Figure 8:

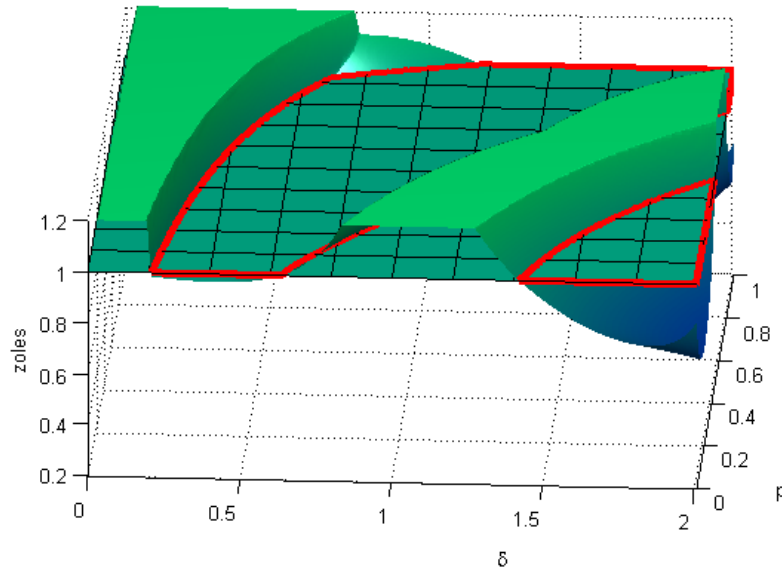


Figure 8. Maximum zero of the BTSHF-DT system VS. sample and hold parameters

With the sample and hold parameter picked within the red region randomly of  $\delta = 0.5$ ,  $p = 0.3$ , the corresponding pole-zero plot of the BTSHF-DT system is shown in Figure 9:

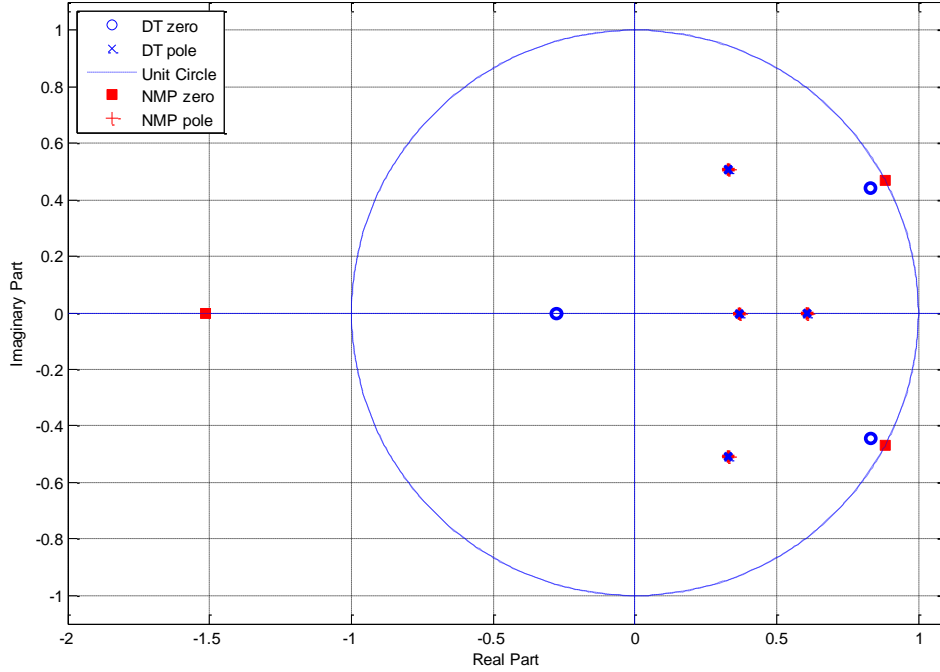


Figure 9. Pole zero plot of the BTSHF-DT system

### 3.4 Analysis

In order to make it clearer, all the feasible regions of the three sample and hold functions are plotted separately and overlapped in Figure 10. It has already been proved that if a combination of the sample and hold parameters are selected within the feasible region, the resulting DT system is MP. In Fig. 10. It depicts the difference between those three regions for each of the sample and hold functions. Also, there are two blue straight dash-dotted lines lies horizontally and vertically representing the fixed sampling rate and duty cycle.

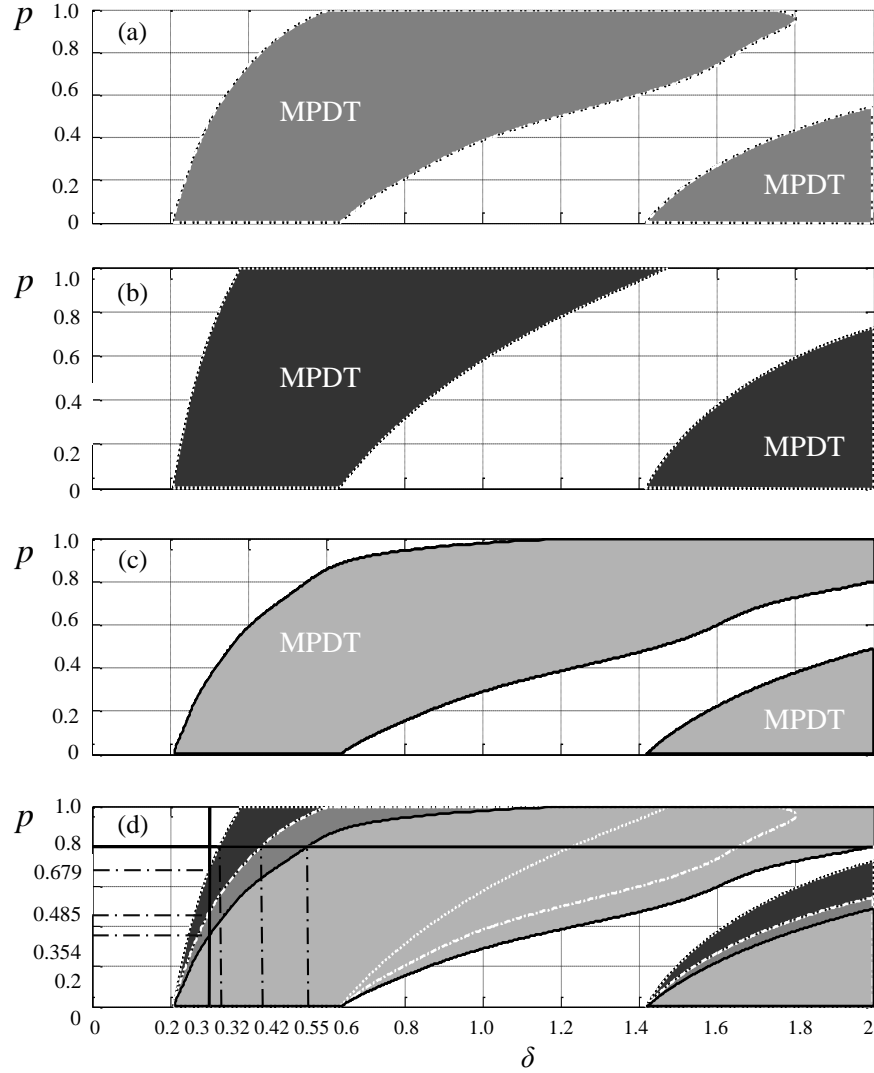


Figure 10. Regions of all the sample and hold functions for selecting the switch parameters so that the resulting DT system is MP

From the result in [9], with ZOH method, the NMP system can also be discretized to MP when the sampling period is sufficiently large. For this system, the zero-order discretizing sampling period varies from 0.60s to 1.76s shown in Figure 10 (a) with the top boundary of the shaded region. Note that this is a special case of the SPSHF at  $p$  is 1.

When  $p$  is at its minimum, which is 0.01 in here, the other sample and hold parameter  $\delta$  are all from 0.2112s, which is the smallest sampling period. This is because when the duty cycle is extremely small, all of the three sample and hold functions converge to a narrow pulse.

From feedback control point of view, the smaller sampling period, the better. For a constant duty cycle, which is 80% in Figure 10 (d), the FTSHF-DT system has the smallest sampling period of 0.3232s, and the BTSHF has the largest sampling period, which is 0.5455s.

From the aspect of energy consumption for actuator, the lower the duty cycle is, the larger magnitude it will be, the more energy it will cost for the actuator to generate the signal. From Fig 10, it is not hard to see that, for a constant sampling period, which is 0.3s, the FTSHF-DT system has the largest duty cycle of 67.9%, then is the SPSHF-DT system, with 48.5% and the BTSHF-DT system has the smallest duty cycle, which is 35.4%. That means the FTSHF input can obtain a higher duty cycle so a lower energy is needed when comparing to the SPSHF and BTSHF cases. From the sample and hold parameter point of view, the FTSHF has the best characteristics among these three sample and hold functions.

No matter which sample and hold function is in use, the  $p$  value cannot reach 0. When  $p \approx 0$ , in each sample period, the input signal has to carry the whole information required in the whole sample period in a significant small time period, which is not be able to actuate.

## CHAPTER 4

### Q-MARKOV COVER IDENTIFICATION USING PRBS INPUT

#### 4.1 Introduction

System identification is a widely used method in modern control. It uses statistical methods to build mathematical models of dynamical systems from measured data. The measured data includes inputs and output (system response). According to the system behavior, system identification considers the original system as a black box, and builds a new system which would have the same response due to the same input. If the input changes due to a noise signal, the system identification can generate a new system due to this changed input signal. Hence, the system identification is used for testing the robustness of this theory. In the next chapter, a CIL simulation with different error is done. After collecting the input and output data, the corresponding DT system is generated by system identification. The robustness is tested by plotting the pole-zero plot to see if the DT system is still MP after adding the error generator. If there is no error generated in the CIL, according to definition 1, the mathematical dynamical model generated by system identification should be a DT system corresponding to the original system, and will have exactly the same poles with the original system. The process and principle of system identification is shown in Fig. 11.

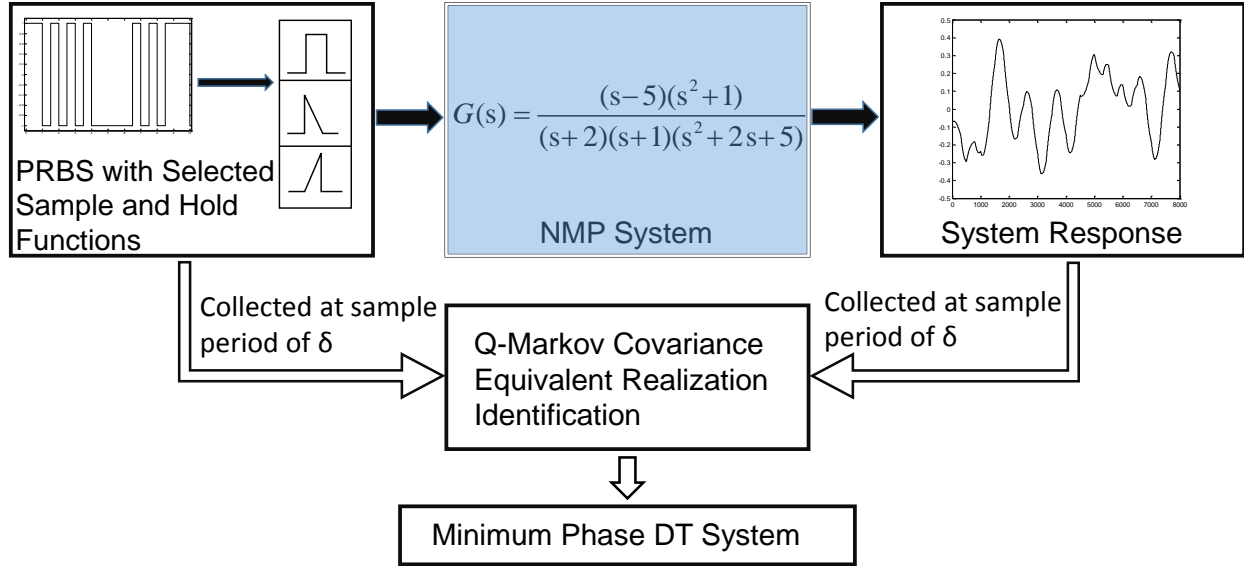


Figure 11. The layout of system identification using PRBS input

Usually, the q-Markov Covariance equivalent Realization method used for identification required white or pulse response ([11] and [12]). But neither of them is a perfect signal.

PRBS is a signal that can be easily generated by shift register circuit. For doing system identification, according to different systems, the order, sampling period and magnitude can be adjusted to have the system well excited. The original q-Markov Cover method for identification required white noise or pulse response [13], which are not perfect input signals. For the white noise, because it is an unrealizable ideal, no signal generators can generate the white noise exactly, hence the identification error is formed at the very beginning of the process. Furthermore it has another huge defect is that it conflicts with saturations on the physical actuators because of its unbounded property. For the pulse response, it is not suitable for all systems because of the limited energy. Consequently, the noise in the process could cover the pulse response for some specific situations. After all of these considerations, the PRBS was used to replace the previous input signals [13].

## 4.2 PRBS Signal

The most commonly used PRBS is based on maximum length sequence (called m-sequence). This type of PRBS is with the length of  $m = 2^n - 1$ , in which  $n$  represents PRBS order. Let  $z^{-1}$  be delay operator and  $\hat{p}(z^{-1})$  be the polynomials [13]

$$\hat{p}(z^{-1}) = a_n z^{-n+1} \oplus \dots \oplus a_2 z^{-1} \oplus a_1 \quad (19)$$

where  $a_i$  is either  $a > 0$  or  $-a$ , and for any number, the calculation of  $a \oplus a$  obeys,

$$1 \oplus 1 = -1 = -1 \oplus -1, \quad 1 \oplus -1 = 1 = -1 \oplus 1 \quad (20)$$

In TABLE 1 [11], lists the selection of coefficients  $a_i$  ( $i = 1, 2, \dots, n$ ) so that  $\hat{p}(z^{-1})$  is obtained to be a maximum sequence. Table 1 is just a part of the whole table in Ref [11], in which the order of greater than 12 and smaller than 34 can be found. In here, order 11 is good enough for doing system identification with this system. The PRBS signal can be generated by the equation shown below:

$$\hat{u}[(k+1)T_p] = \hat{p}(z^{-1})\hat{u}(kT_p), \quad k = 0, 1, 2, \dots, \quad (21)$$

where  $\hat{u}(0) = 1$  and  $\hat{u}(-1T_s) = \hat{u}(-2T_s) = \dots = \hat{u}(-nT_s) = 0$ , in where  $T_s$  is the PRBS generating rate.

For q-Markov Cover use, the PRBS need to be inversed, and the inversed PRBS is calculated as

$$u(k) = s(k) \oplus [-a + 2a \hat{u}(k)], \quad s(k) = \begin{cases} a & k \text{ even} \\ -a & k \text{ odd} \end{cases} \quad (22)$$

in which  $u(k)$  has a period of  $2m$  and  $u(k) = -u(k+m)$ . The mean of the inverse PRBS is

$$m_u = E_{2m}(kT_p) = \frac{1}{2m} \sum_{i=0}^{2m-1} u(kT_p) = 0 \quad (23)$$

TABLE 1. Coefficients for maximum sequences

Order of Polynomial $n$	Period of the sequence $m$	Non-negative coefficients $a_i$
2	3	$a_1, a_2$
3	7	$a_2, a_3$
4	15	$a_3, a_4$
5	31	$a_3, a_5$
6	63	$a_5, a_6$
7	127	$a_4, a_7$
8	255	$a_2, a_3, a_4, a_8$
9	511	$a_5, a_9$
10	1023	$a_7, a_{10}$
11	2047	$a_9, a_{11}$

Since the inversed PRBS signal is the only thing used for q-Markov Cover system identification, in the following of this thesis, “PRBS” stands for inversed PRBS. A part of the PRBS signal with the order of 11 is shown in Figure 12:



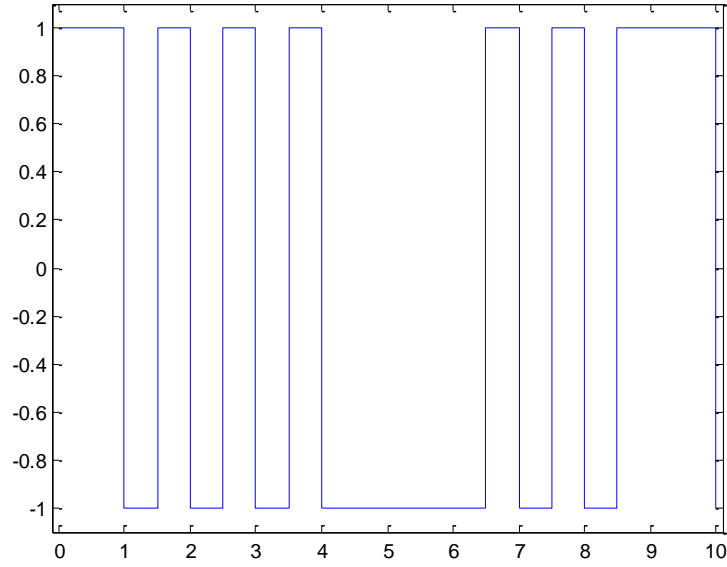


Figure 12. Several periods of PRBS signal with the order of 11

In Figure 13, it is the modified PRBS signal, which is combining PRBS and the ZOSHF and the three switched sample and hold functions. The first plot is the PRBS signal combined with ZOSHF. The second plot is the PRBS combined with SPSHF, the third is combined with FTSHF, and the last one is combined with BTSHF.

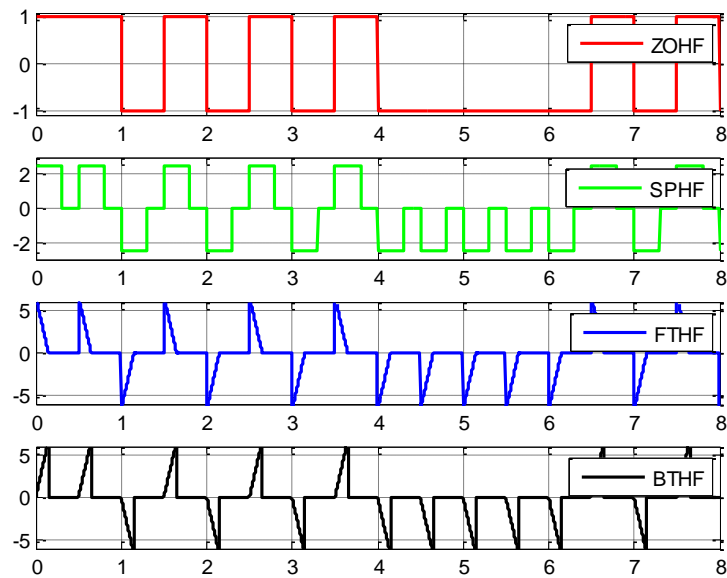


Figure 13. The modified PRBS signal

The sample and hold parameters are selected according to the former section to make sure that the resulting DT system is MP. Due to the different input signals, the NMP system response are different and shown in Figure 14.

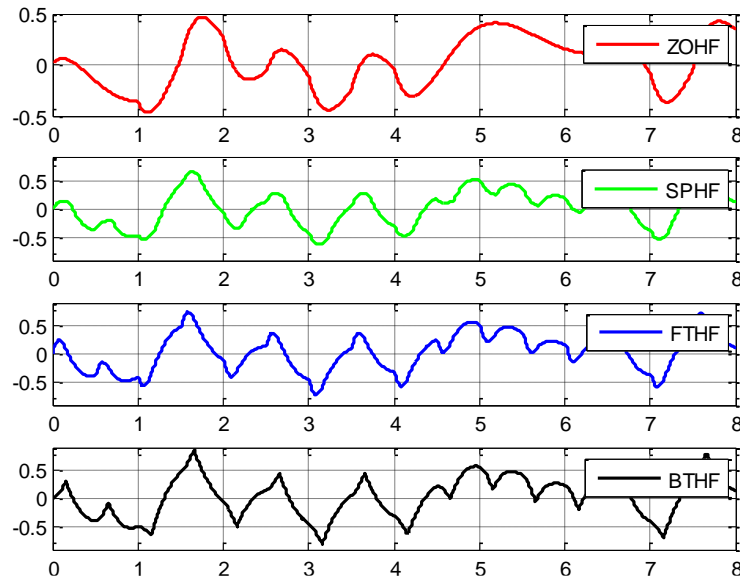


Figure 14 System response due to different inputs

### 4.3 System Identification

In this thesis, the system identification is done by using a Matlab GUI file [14]. The PRBS GUI was developed by Dr. Guoming Zhu for multi-rate PRBS q-Markov Cover. The number of Markov parameters besides the order of the identified system model can be adjusted by using the system identification GUI.

#### 4.3.1 System Identification Steps

There are three steps of doing the system identification with PRBS and its parameter selection:

### Step1: Design the PRBS system identification

To design the experiment, according to parameter  $m$ , the magnitude and the order of the PRBS signals need to be determined first. Usually, the magnitude of PRBS is determined by choosing the most feasible number so that the ratio of system output signal to noise signal is maximized. The order of PRBS is chosen based on covering the dominated frequencies of the identified system such that the identified system could be excited by PRBS signal. Also, the output sample period  $T$  need to be determined secondly, which is basing on the actuator response to PRBS signal.

### Step 2: Run the system identification test and collect data

After all the necessary parameters are determined, the next step is to run and collect both input and output (system response) data. In order to achieve an accurate system response, a steady state response is required, which means that for a certain system, the tenth cycle or more could be used for data collection.

### Step 3: Run the GUI to do the system identification

Convert all the data collected in the last section to a Matlab data file. The PRBS system identification GUI can be used to obtain a linearized system model. During the use of GUI, the output weighting matrix  $Q$ ,  $q$  of Markov and covariance parameter are need to be determined. The parameters are determined based on different identification systems. The weighting matrix is used for balancing the output response scale for different output channels. The  $q$  of Markov is used for adjusting the identification result by telling how well the identified model response matches the original system response.

### 4.3.2 System Identification Parameter Determination

The order of the PRBS signal is set to be 11, so that the length is enough to excite the system to do the system identification. Since the PRBS signal will be combined with the sample and hold functions, and the magnitude is set to be 1. With these two parameters (order and magnitude), the PRBS can be generated by a Matlab m file. With the signal, a Simulink file could be established. In the Simulink, the sample period of PRBS has to match with the sample and hold function's sample period, which is set to 0.5s for each sample and hold function. The duty cycle of each sample and hold function is set the same as the  $p$  in last chapter. Since the bandwidth of the system is 21.23Hz, according to Shannon-Hartley's theorem [15], the smallest simulation step size is determined to be 0.016s. So in here, during the simulation, the simulation step size is set to be 0.001s.

The following figure is the Simulink layout for achieving the system output by inputting a PRBS signal.

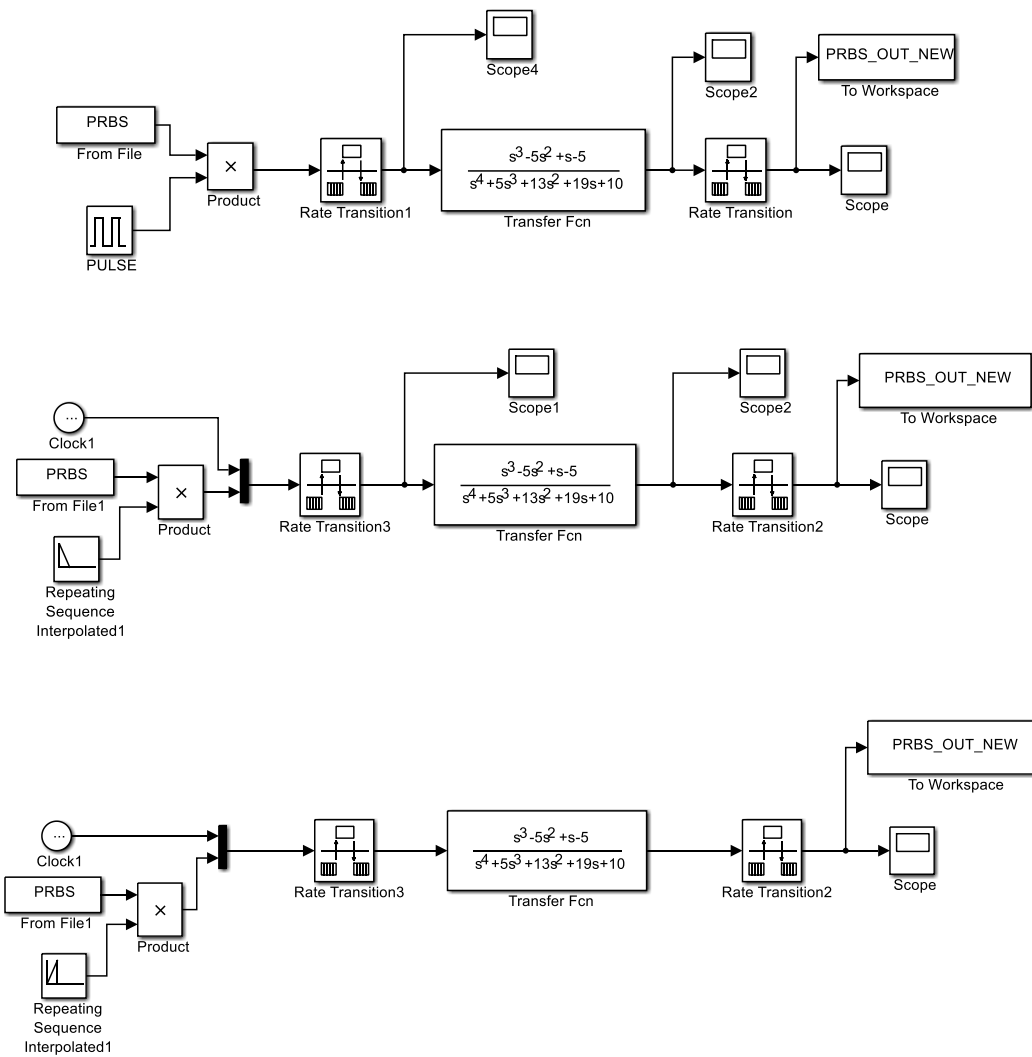


Figure 15. Simulation layout

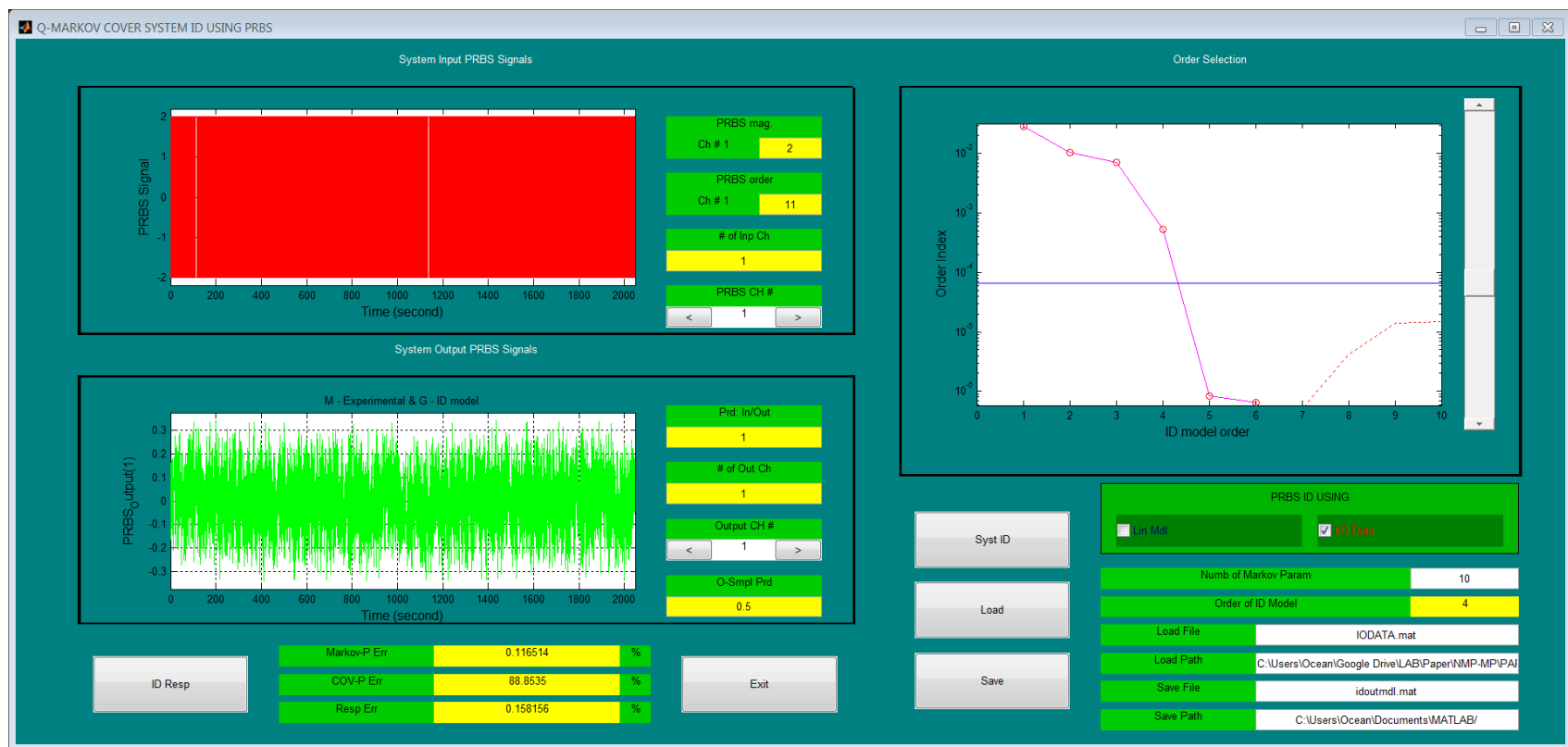


Figure 16. System Identification GUI

After running the Simulink, the output data including the modified input signal and the system response signal are collected both at sampling period of 0.5s, which is the same as the switched input sampling periods, and imported to the system identification GUI. In the GUI, the number of Markov parameter is set to be 30 and the order of the identified model is 4 for a better identification result. The identified system is then achieved.

#### 4.3.3 Identified Result of the SPSHF Case

Since the input and output data were collected at the fixed sampling time of 0.5s, the identified system was in discrete time domain. According to Figure 3 and Figure 9, the sample and hold parameters were set to  $\delta = 0.5$ ,  $p = 0.4$ , because in Figure 3, this set of sample and hold parameters made the maximum absolute zero of the SPSHF-DT system under the plane of  $z = 1$ , so that the DT system was MP. The system identification result is shown in Figure 1.

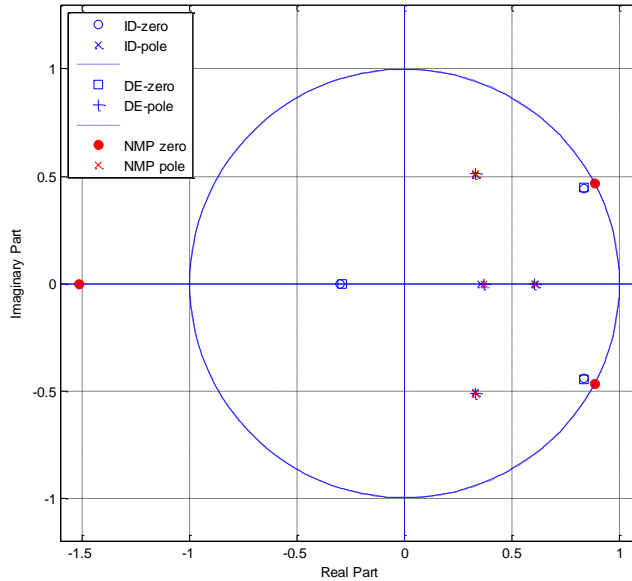


Figure 17. The pole-zero plot of SPSHF-DT, identified and NMP systems

In the following table, the numerical poles and zeroes of Figure 17 are listed.

TABLE 2. The pole and zero absolute value of the SPSHF-DT case

IDENTIFIED POLE	DT POLE	IDENTIFIED ZERO	DT ZERO
0.6069	0.6065	0.9456	0.9458
0.6069	0.6065	0.9456	0.9458
0.6117	0.6065	0.4501	0.4455
0.3539	0.3679		

#### 4.3.4 Identified Result of the FTSHF Case

The sample and hold parameters were selected to be  $\delta = 0.5$ ,  $p = 0.3$  for the FTSHF case. The result of system identification is shown in Figure 18.

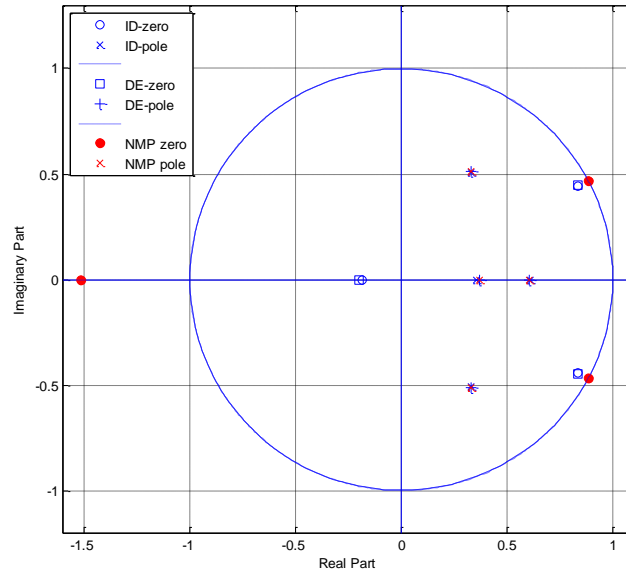


Figure 18. The pole-zero plot of FTSHF-DT, Identified and NMP

In the following table, the numerical poles and zeroes of Figure 18 are listed.



TABLE 3. The pole and zero absolute value of the FTSHF-DT case

IDENTIFIED POLE	DT POLE	IDENTIFIED ZERO	DT ZERO
0.6081	0.6065	0.9528	0.9537
0.6081	0.6065	0.9528	0.9537
0.6209	0.6065	0.2082	0.1899
0.3247	0.3679		

#### 4.3.5 Identified Result of the BTSHF Case

By applying the same process, the system identification result of BTSHF with  $\delta = 0.5$ ,  $p = 0.3$  is in Figure 19 and Table 4.

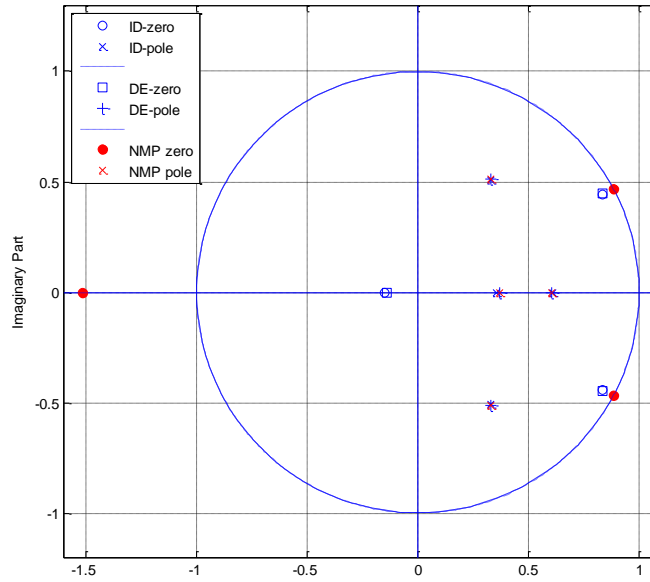


Figure 19. The pole-zero plot of BTSHF-DT, identified and NMP systems

And the poles and zeroes are shown in the following table:

TABLE 4. The pole and zero absolute value of the BTSHF-DT case

IDENTIFIED POLE	DT POLE	IDENTIFIED ZERO	DT ZERO
0.6074	0.6065	0.9407	0.9425
0.6074	0.6065	0.9407	0.9425
0.6161	0.6065	0.3080	0.2789
0.3415	0.3679		

From the three figures and the tables list in this section, the poles and the zeroes of the identified system generated by the system identification match with the calculated DT system perfectly with the same sample and hold parameters, which means that the system identification can identify the system precisely and it is good for doing CIL simulation.

#### 4.4 DE System GUI for Finding the MPDT Systems

##### 4.4.1 Introduction

In order to make the calculation process faster and more convenient, a GUI was made for finding the DT systems according to SPSHF, FTSHF and BTSHF. 3-D plots and 2-D plots are made for observing the feasible regions for selecting sample and hold parameters so that the resulting DT system is MP.

The DE GUI layout is shown in Figure 20. It consists five buttons, five figures and two tables. The buttons are “Load System”, “RUN”, “Save”, “Parameter Selection” and “Achieve MP”. The figures are “original pole-zero plot”, “holding function plot”, “3D plot of the holding parameter

VS. system zeroes”, “Feasible parameter area plot”, and “DT pole-zero plot”. The two tables are used for displaying the poles and zeroes of the corresponding DT system.

#### 4.4.2 Procedure

The “Load System” button is used for loading an external transfer function with the form of a Matlab data file into the GUI system. The transfer function could be either NMP or MP, the GUI will tell which sort of system it is and respond correctly.

After input the system transfer function, a sample and hold method should be chosen by using the pop up menu. Three sample and hold function options are listed in the pop up menu, which are “Pulse”, “Forward Triangle” and “Backward Triangle”. Once a sample and hold method is selected, the general picture of the sample and hold function will appear in the figure on the up right corner.

Then, the “RUN” button should be clicked for plotting the 3D plot of the sample and hold parameter VS. system zeroes. After clicking, it will take a while for Matlab calculating the matrix and plot it out. The 3D plot is the first overlook of choosing the sample and hold parameters.

In order to make it clearer, the “Parameter Selection” button is used for plotting the feasible sample and hold parameter area (green portion). By using the two slid bar (horizontal one is used for choosing  $\delta$ , and the vertical one is for choosing  $p$ ), the feasible sample and hold parameters are selected. When the bar moves, the corresponding parameter value will appear in the text box in the middle. The cross section of those two red lines represents the sample and hold parameter combination. So if the cross section is inside the green area, the outcome DT

system of the GUI will be MP. The desired sample and hold parameter could also be selected by inputting directly into the edit box, which will also affect the slider bar position.

“Achieve MP” button is used for plotting the pole-zero plot of the achieved DT system. Once it is clicked, the pole-zero plot will appear in the “DT pole-zero plot” figure. At the same time, the poles and zeroes of the DT system will appear in those two tables also with their absolute value. By looking at this figure or the tables, the characteristic of the DT system could be observed.

At last, all the results including the original system, original pole and zero, sample and hold method, sample and hold parameters, and the DE system will be saved automatically by clicking the “Save” button. All the result will saved in a single Matlab data file in the same directory with the loaded system file.

#### **4.4.3 Benefits**

This GUI has five benefits:

1. It becomes easier to identify a system is a MP or NMP. Simply input the system into the GUI, and look at the first figure —“original pole-zero plot”.
2. It becomes faster to tell if a system has its MPDT or not by looking at the 3D plot or the “Feasible parameter area plot”. If there is a certain area under the  $z = 0$  plan, it means that the system has its MPDT system.
3. It is much faster to find the DT system
4. The choice of finding DT system is visual and adjustable

#### **4.4.4 Future work of the DE GUI**

1. The higher the order of the system is, the longer time the calculation needs. Due to the problem of long time calculation, the Matlab code could be optimized to achieve the results in a shorter time.
2. The color of the outlook could be optimized in order to make the result clearer.
3. A new portion could be developed to show the transfer function of the DT system.
4. The boundary of the feasible area should be plotted in order to show the area clearer.

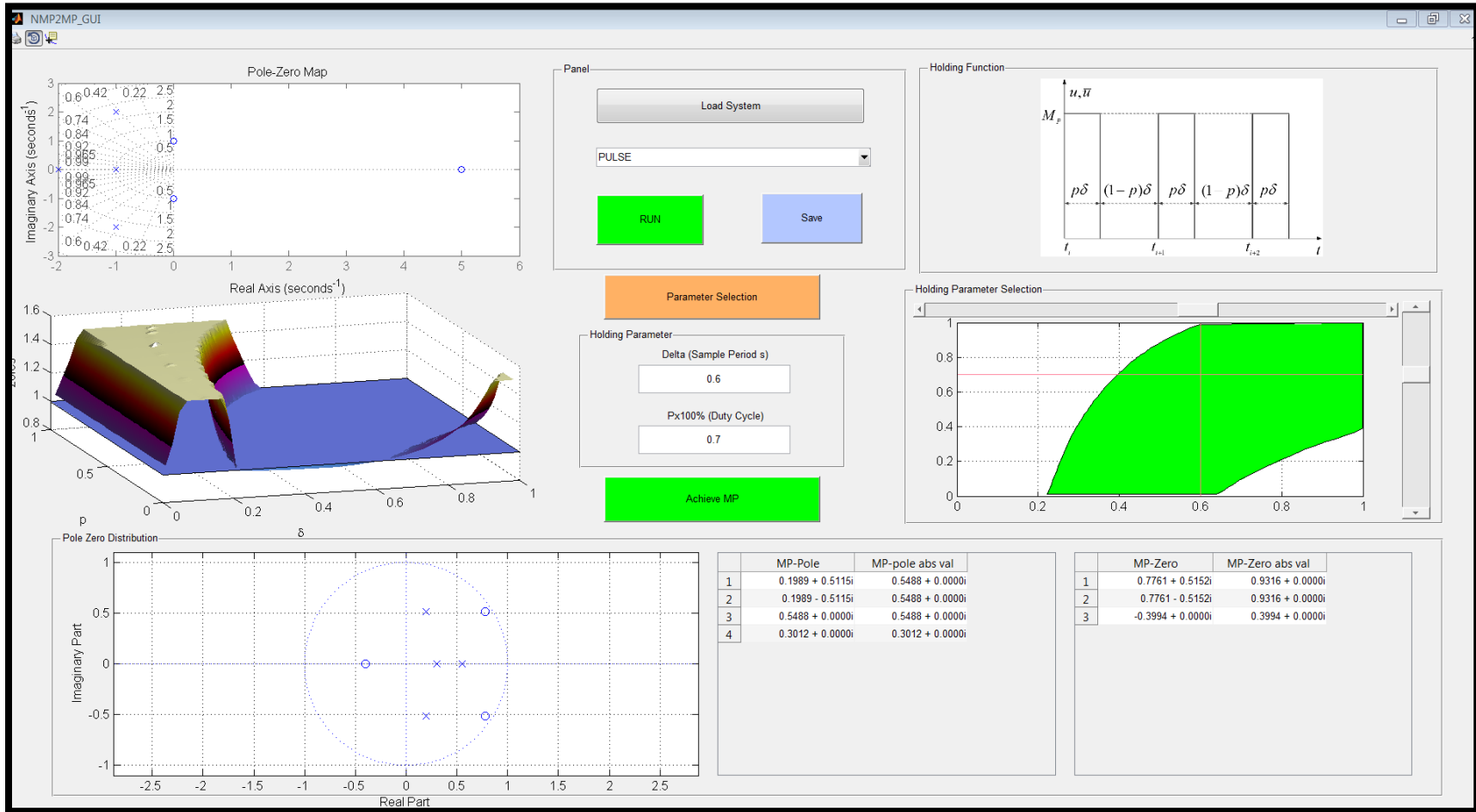


Figure 20. The GUI for finding the MPDT system

## CHAPTER 5

### CIL SIMULATION USING A DSPACE AUTO-BOX

#### 5.1 Introduction

In this thesis, the dSPACE auto-box and a RC filter were connected to the system to perform as real-time simulation in the CIL system. dSPACE was responsible for all the calculation processes including the system dynamics and the modified PRBS input signal. Also, in order to test the robustness of this theory, an adjustable RC filter was connected with the dSPACE auto-box to simulate actuator dynamics using different capacitors. The system Simulink model and the signal generating file were built in the main CPU board in the dSPACE. The control signal was sampled and held in dSPACE, output by the D/A board, filtered by the circuit and input to dSPACE by A/D board.

In Figure 21 and Figure 22, the flowchart and the actual layout of the whole process are showed. After the CIL simulation was conducted, the modified PRBS input and the corresponding system output data were collected both at the sampling period of  $\delta$  (0.5s). With the collected data, the system identification was conducted and form the corresponding identified systems. Comparing the different identified systems due to the change of capacitors of the RC filter with the MPDT system, the results of robustness test could be observed.

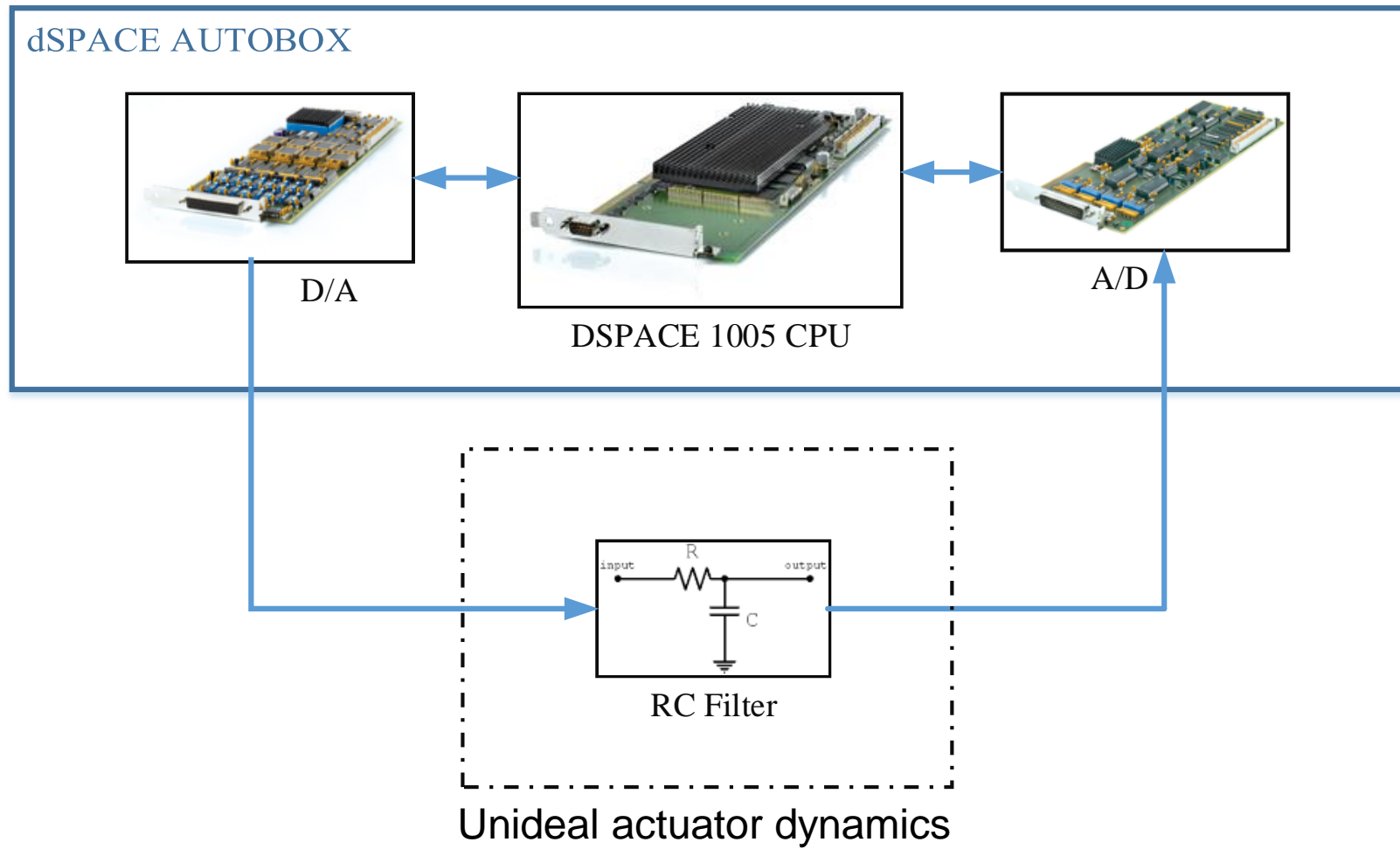


Figure 21. The flowchart of CIL Simulation



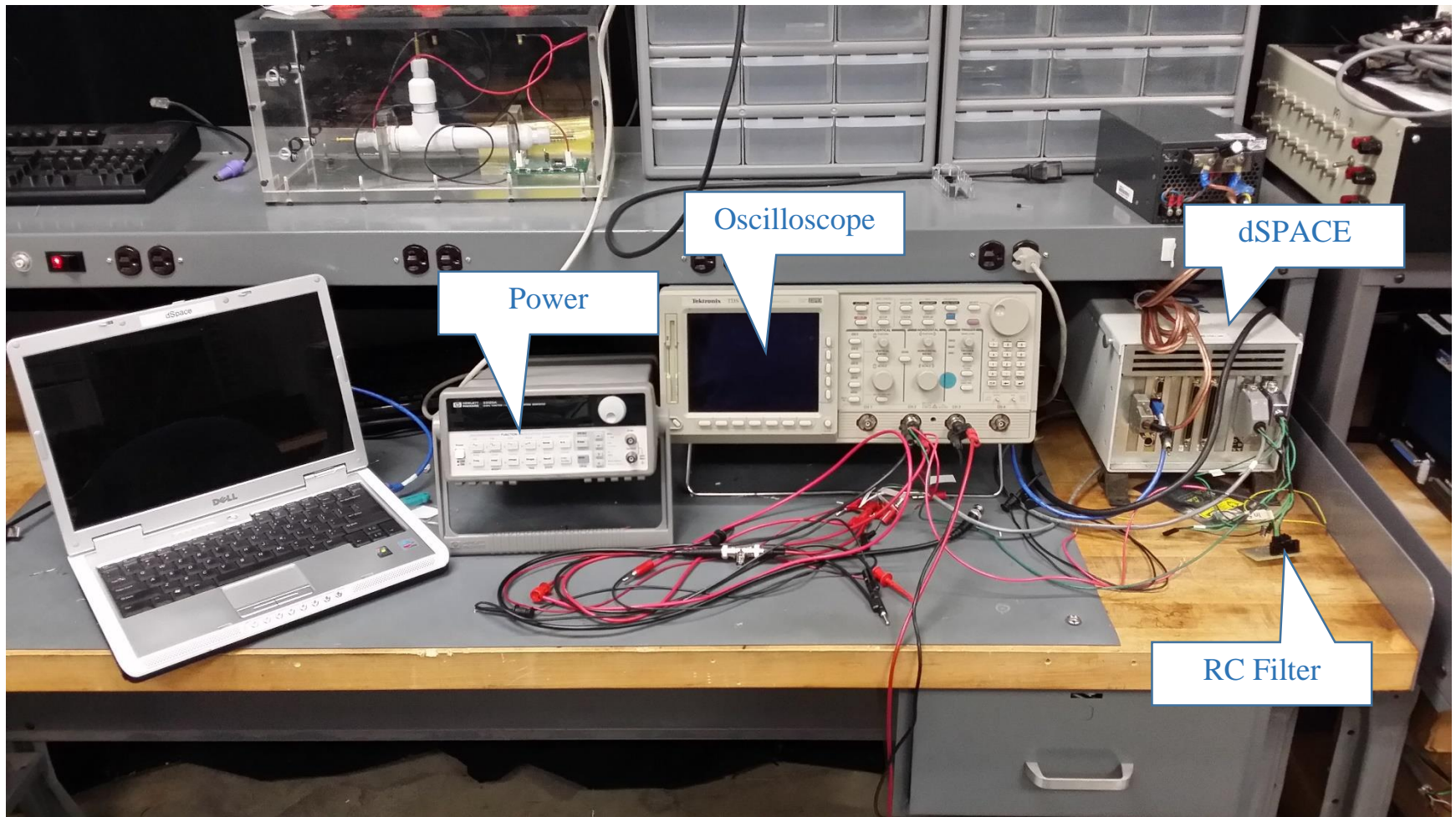


Figure 22. dSPACE setup

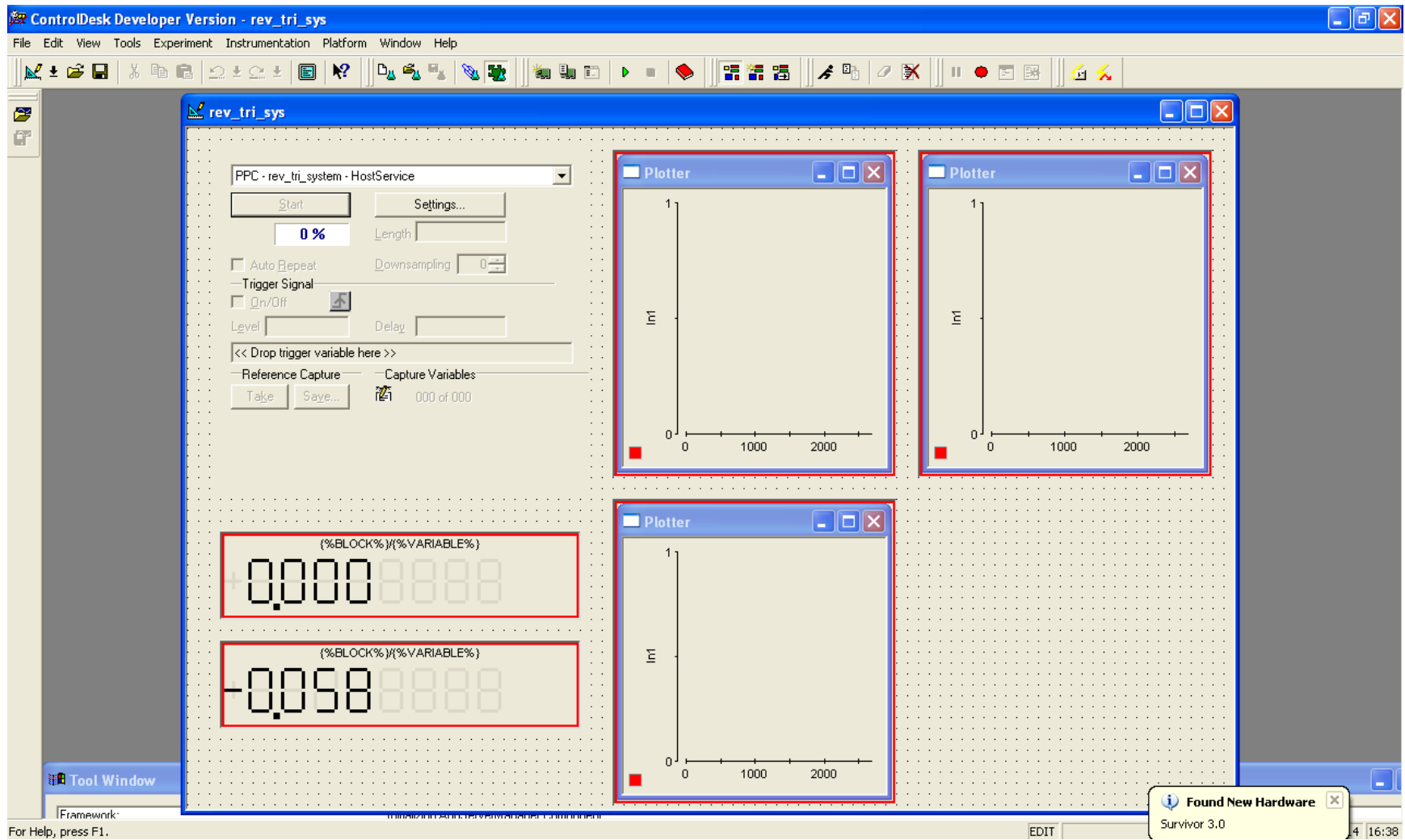


Figure 23. dSPACE control desk layout

## 5.2 RC Filter

As shown in figure 21, the RC filter was a simple resistance-capacitor circuit. To be an adjustable RC filter, the resistance was fixed at  $1\text{k}\Omega$ , and the capacitors used in this experiment were  $1\ \mu\text{F}$ ,  $3.3\ \mu\text{F}$ ,  $10\ \mu\text{F}$ ,  $47\ \mu\text{F}$ , and  $100\ \mu\text{F}$ . The system was simulated using each value of the capacitor to have different system responses.

During the simulation, the capacitor would discharge its stored energy through the resistor. By applying Kirchhoff's voltage equation [16], yielding(24).

$$V_1(s) = (R + \frac{1}{Cs})I(s) \quad (24)$$

And the output voltage is

$$V_2(s) = I(s)(\frac{1}{Cs}) \quad (25)$$

Therefore, solving (24) for  $I(s)$  and substituting into(25):

$$V_2(s) = \frac{(1/Cs)V_1(s)}{R + 1/Cs} \quad (26)$$

Then the transfer function is obtained:

$$G(s) = \frac{V_2(s)}{V_1(s)} = \frac{1}{RCs + 1} = \frac{1}{\tau s + 1} \quad (27)$$

$\tau$  is the time constant of the network. With different capacitance, the time constant and the pole of equation (32) in continuous time domain are shown in Table 5.

TABLE 5. Time constant VS. pole locations

TIME CONSTANT (S)	POLE
0.001	-1000
0.0033	-303
0.01	-100
0.047	-21.27
0.1	-10

The poles of the original system in the numerical simulation section were  $-2, -1, -1 + 2i, -1 - 2i$ , the RC transfer function poles were too small when comparing with the original system poles. As a result, the RC filter poles were ignored as a part of the transfer function due to the 0.001 simulation step length, instead, it was only been considered as an error, or noise. The modified PRBS signal changed due to different capacitors are shown in Figure 24.

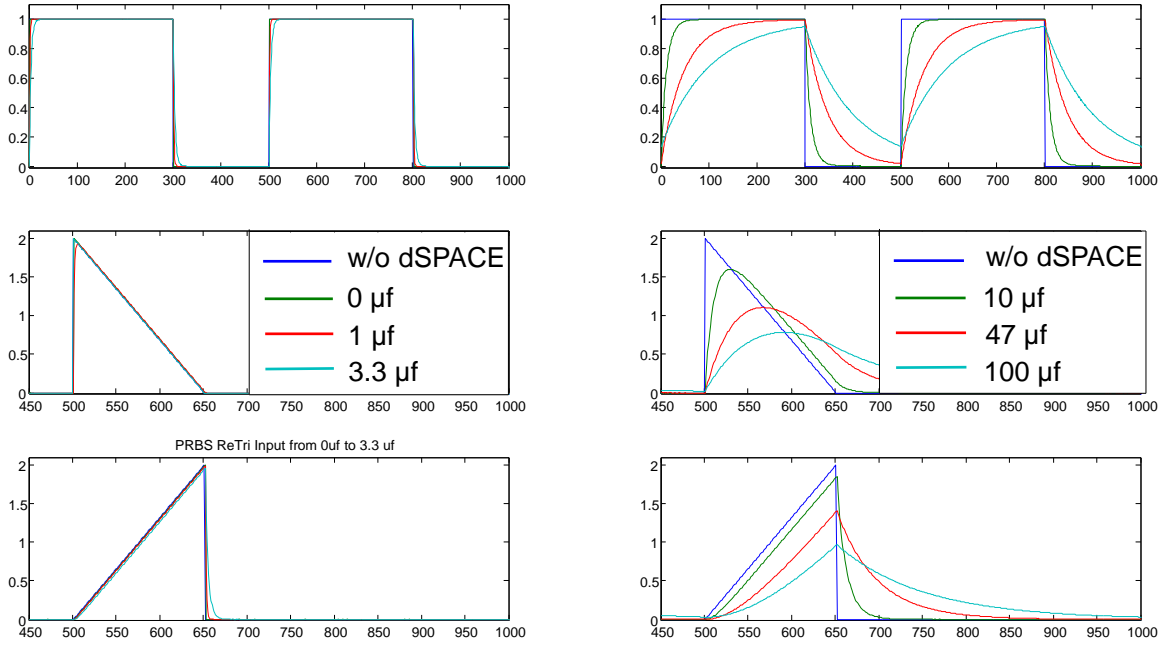


Figure 24. The modified PRBS input signal

From figure 24, it was obvious that when the capacitance was increasing, the modified input becomes smoother and the magnitudes were smaller.

### 5.3 CIL Result

Due to the change of the input signal, the system response will definitely change. As a result of observation, as the capacitor was increasing, the outcome of the system identification was changing by moving the locations of the zeroes towards to a NMP direction (outside of the unit circle). The simulation results of SPSHF-DT, FTSHF-DT and BTSHF-DT systems are shown in Figure 25, Figure 26, and Figure 27.

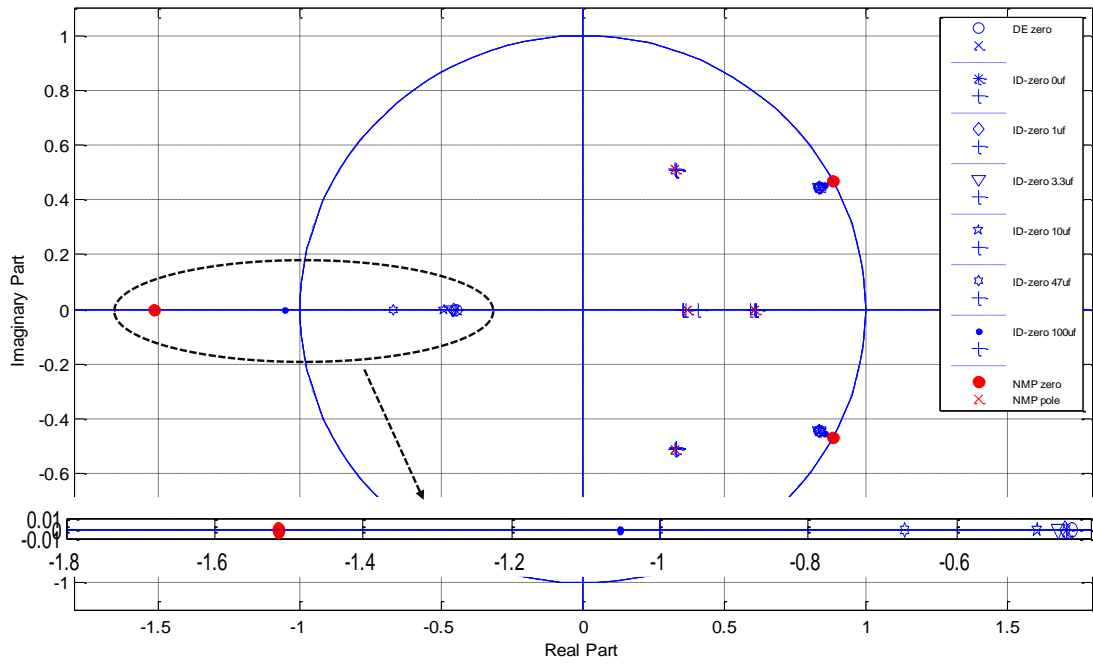


Figure 25. The zero moving trend of the identified system with SPSHF

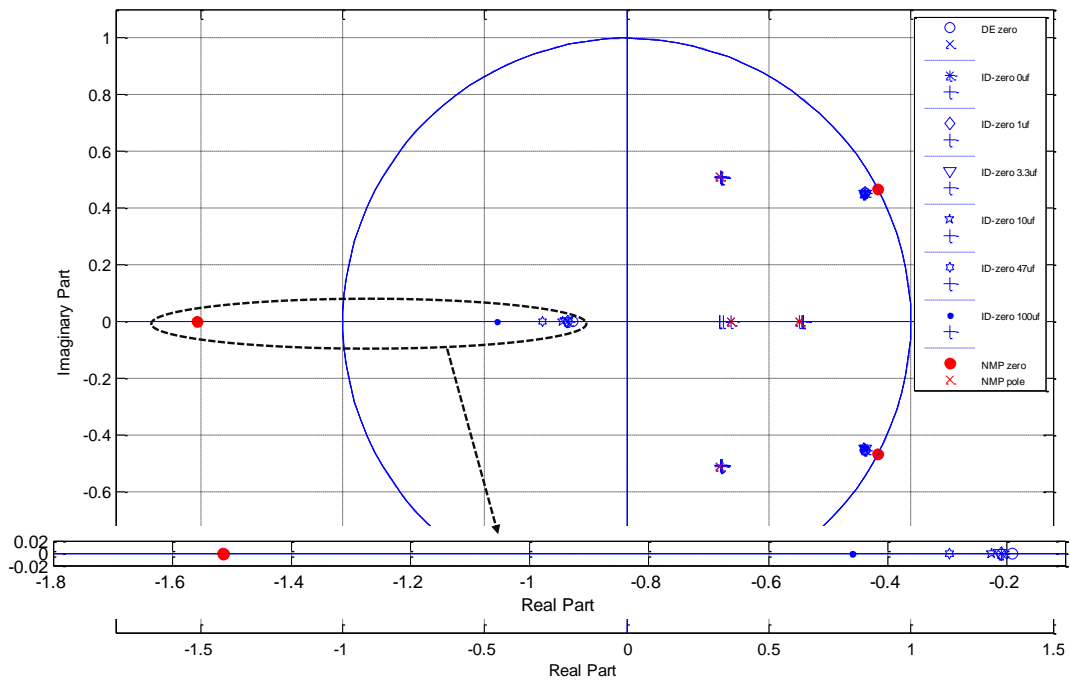


Figure 26. The zero moving trend of the identified system with FTSHF

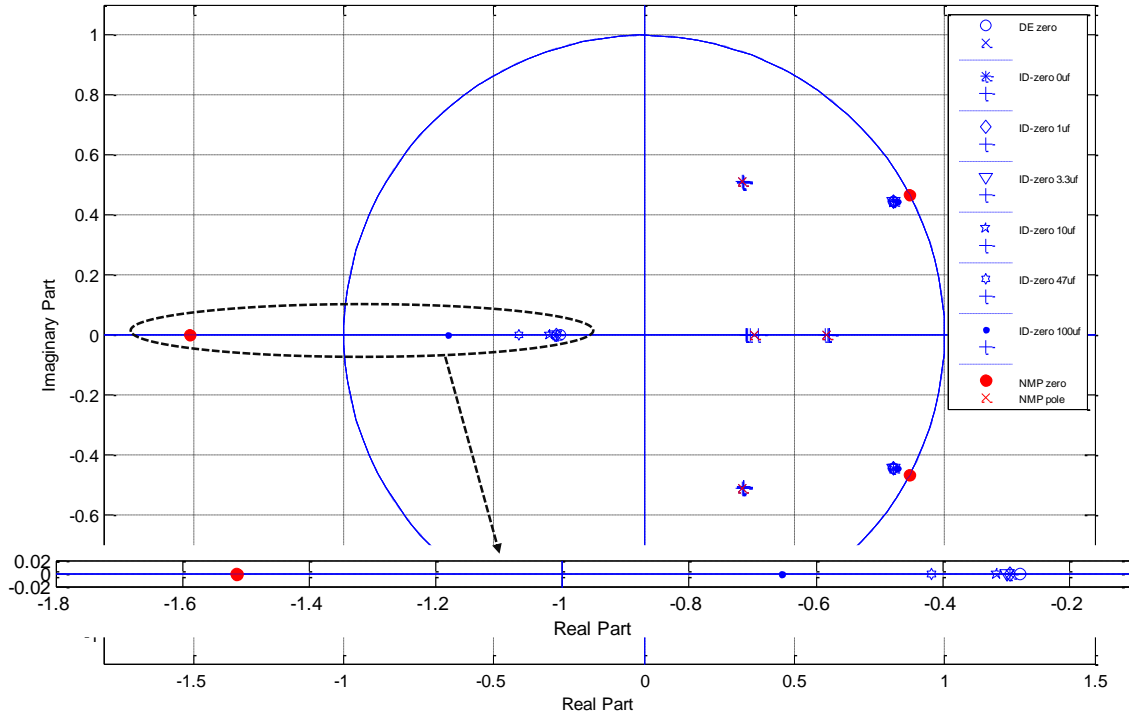


Figure 27. The zero moving trend of the identified system with BTSHF

## 5.4 Analysis

From the CIL result figures, it is clear that for all of the three sample and hold functions, the negative zero moving trend was the most significant and they would become smaller than  $-1$  at a certain capacitance value. In this experiment, when the capacitance reached  $100 \mu F$ , only the negative zero of the SPSHF became smaller than  $-1$ .

For the purpose of comparing the robustness of all the sample and hold functions, the zero moving trends of the three sample and hold functions are plotted in Figure 28. The vertical value of the plot is the difference between the new identified systems negative zero and the original MPDT negative zero.

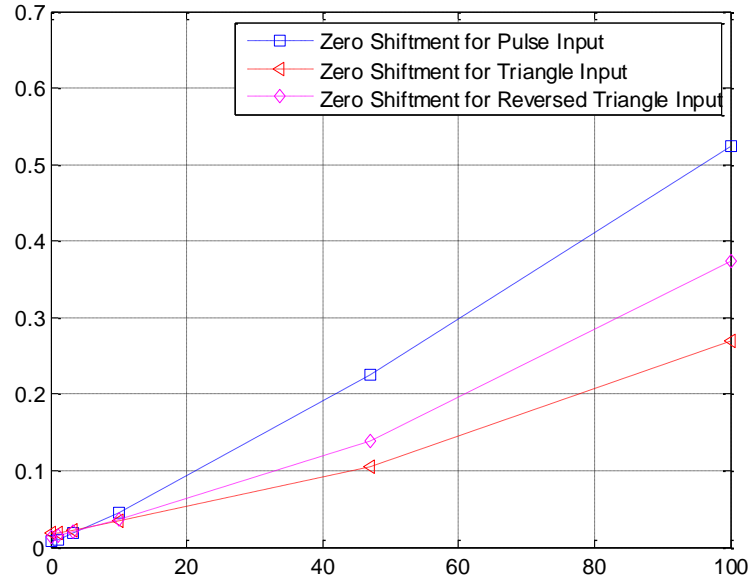


Figure 28. Overall zero moving trends of the three sample and hold functions

From Figure 28, only the SPSHF-DT system become NMP when the capacitance of the RC filter reached  $100 \mu F$ . The moving trends of the other two sample and hold method were smaller than the SPSHF. The smallest was the FTSHF, which means that the FTSHF method had the best robustness.



## CHAPTER 6

### CONSLUSIONS

A new way of studying a NMP system was discovered by a previous work, which was focusing on finding the DE system of a NMP system. The DE system with a ZOSHF input would have exactly the same response with a NMP system with a switched input at sampling times. The switched input used here was defined as SPSHF and the DE system state space matrices equation was developed by equaling the sate variables of the DE system and the NMP system at sampling times. And it was also proved that with a proper choice of the sample and hold parameters, the corresponding DE system could be MP.

In this thesis, the definition of the switched input was expanded with another two sample and hold functions, which were FTSHF and BTSHF. Followed the same steps of finding the DE system in the previous work, the DE system state space equations of the FTSHF case and BTSHF case were developed. A New definition called DT system was introduced by discretizing the DE systems. For each case, the feasible combinations of the sample and hold parameters for achieving MP characteristics were studied. 3D figures were plotted for indicating the relationship between the sample and hold parameters and the maximum absolute zero of the corresponding DT systems. When comparing the feasible regions for selecting the sample and hold parameters, the FTSHF had the better choices (larger region) of a smaller sampling period and a larger duty cycle. Also comparing with the zero-order discretizing, smaller sampling period was achieved for the MP DT system.

The robustness study was completed using CIL simulations with the help of system identification. After doing the CIL simulation, the results showed that the SPSHF has the worst

robustness with increased actuator modeling error; while FTSHF provided the best robustness among the three sample and hold functions.

As a summary, the best sample and hold function is the FTSHF due to its robustness property with the largest feasible sample and hold parameter region.

## **BIBLIOGRAPHY**

## BIBLIOGRAPHY

- [1] S. Zhao and Z. Gao, “Active disturbance rejection control for non-minimum phase systems,” *Proceedings of the 29<sup>th</sup> Chinese Control Conference*, July, 2010.
- [2] Tzuu-Hseng S. Li, and Ming-Yuan Shieh, “Design of a GA-based fuzzy PID controller for non-minimum phase systems” *Fuzzy Sets and Systems* volume 111, issue 2 , 2000, pp. 183-197.
- [3] C.-Y. Tsai, T.-H.S. Li, “Fuzzy logic control of nonminimum phase system”, *Proc. FUZZ-IEEE'94*, June 1994, Orlando, FL, USA, pp. 199-204
- [4] S. Park, L.J. Park, C.H. Park, “A neuro-genetic controller for nonminimum phase systems” *IEEE Trans. Neural Networks*, pp. 1297–1300, 1995
- [5] H. Elliott, “Direct adaptive pole placement with application to nonminimum phase systems” *IEEE Trans. Automat. Control*, AC-27 pp. 720–721, 1987
- [6] L. Parly, “Towards a globally stable direct adaptive control scheme for not necessarily minimum phase systems”, *IEEE Trans. Automat. Control* AC-29 pp. 946-949. 1984
- [7] G. Bartolini, T. Zolezzi, “The V.S.S. approach to the model reference control of nonminimum phase linear plants”, *IEEE Trans. Automat. Control* AC-33, pp. 859-863, 1988
- [8] Rouhollah Jafari and Ranjan Mukherjee, “Intermittent Output Tracking for Linear Single-Input Single-Output Non-Minimum-Phase Systems,” *ACC* June 27-June 29 2012
- [9] G. Bartolini, A. Ferrara, “Variable structure approach to the pole assignment control of nonminimum phase systems”, *Internat. J. Control* 57 pp. 1063-1078, 1993
- [10] T. Das and R. Mukherjee, “Shared-sensing and control using reversible transducers,” *IEEE Transactions on Control Systems Technology*, vol. 17, no. 1, pp. 242–248, 2009.
- [11] A.M King, U. B. Desai, and R.E Skelton. “A generalized approach to q-Markov covariance equivalent realizations of discrete systems.” *Automatica*, 24(4), 1988
- [12] K. Liu, R. E. Skelton. “Identification and control of NASA’s ACES structure. In *Proceedings of American Control Conference*”, Boston, MA, Jun 1991.
- [13] G. Zhu, “Weighted multirate q-Markov Cover identification using PRBS – an application to engine systems,” *Mathematical Problems in Engineering*, Vol. 6, pp. 201-224, 2000.

- [14] Guoming Zhu, Robert E. Skelton and Pingkang Li, "Q-markov Cover Identification Using Pseudo random binary Signals" International Jurnal of Control, Vol. 62, pp. 1273-1290, 1995
- [15] Eric Price, David P. Woodruff, "Applications of the Shannon-Hartley Theorem to Data Streams and Sparse Recovery " IEEE International Symposium on Information Theory Proceedings pp 2446-2450 1-6 july 2012
- [16] Richard C. Dorf Robert H. Bishop, "Modern Control Systems," pp. 65-66,2011